big data and cognitive computing

MDPI

Article

Predicting Intensive Care Unit Admissions in COVID-19 Patients: An AI-Powered Machine Learning Model

A. M. Mutawa [1,2]

[1] Computer Engineering Department, Kuwait University, Safat 13060, Kuwait; dr.mutawa@ku.edu.kw
[2] Computer Sciences Department, University of Hamburg, 22527 Hamburg, Germany

Abstract: Intensive Care Units (ICUs) have been in great demand worldwide since the COVID-19 pandemic, necessitating organized allocation. The spike in critical care patients has overloaded ICUs, which along with prolonged hospitalizations, has increased workload for medical personnel and lead to a significant shortage of resources. The study aimed to improve resource management by quickly and accurately identifying patients who need ICU admission. We designed an intelligent decision support system that employs machine learning (ML) to anticipate COVID-19 ICU admissions in Kuwait. Our algorithm examines several clinical and demographic characteristics to identify high-risk individuals early in illness diagnosis. We used 4399 patients to identify ICU admission with predictors such as shortness of breath, high D-dimer values, and abnormal chest X-rays. Any data imbalance was addressed by employing cross-validation along with the Synthetic Minority Oversampling Technique (SMOTE), the feature selection was refined using backward elimination, and the model interpretability was improved using Shapley Additive Explanations (SHAP). We employed various ML classifiers, including support vector machines (SVM). The SVM model surpasses all other models in terms of precision (0.99) and area under curve (AUC, 0.91). This study investigated the healthcare process during a pandemic, facilitating ML-based decision-making solutions to confront healthcare problems.

Keywords: COVID-19; feature selection; intensive care unit; machine learning; SMOTE; SHAP

Academic Editors: Hossein Hassani and Steve MacFeely

Received: 20 November 2024
Revised: 29 December 2024
Accepted: 10 January 2025
Published: 14 January 2025

Citation: Mutawa, A.M. Predicting Intensive Care Unit Admissions in COVID-19 Patients: An AI-Powered Machine Learning Model. *Big Data Cogn. Comput.* **2025**, *9*, 13. https://doi.org/10.3390/bdcc9010013

1. Introduction

The COVID-19 pandemic has led to an unprecedented crisis among the human fraternity across the globe in terms of mortality, morbidity, and economic impact. Of the 576.58 million COVID-19 cases registered globally as of 25 July 2022, 6.4 million people died of the virus [1]. Identifying and targeting those at the highest risk became crucial for effectively allocating inadequate medical resources [2]. Infectious illness outbreaks can be predicted at times, but there is always ambiguity about their precise nature. As such, the resources and knowledge gained while dealing with the COVID-19 pandemic are still relevant, even though the immediate danger may have subsided. The strategic methodologies honed during this recent disaster can help to overcome future health emergencies. Research conducted during the COVID-19 pandemic aimed to enhance awareness within the healthcare community and address unforeseen challenges. The advanced predictive models, cutting-edge techniques, and strategic perspectives developed can serve as crucial tools for handling health crises in the future.

The data management, predictive analytics, and strategic knowledge skills acquired over this period may be efficiently repurposed to tackle various illnesses and also to

mitigate healthcare emergencies [3]. In this context, age, preexisting medical disorders, and lack of vaccination are significant factors exacerbating viral severity in people [4].

An intensive care unit (ICU) is a specialist critical care unit intended to treat and manage patients with life-threatening diseases. Admission policies for older adults in ICUs are carefully considered to improve treatment outcomes and reduce mortality rates in this population [5]. Research by Olds et al. highlights the need for improved interaction and translation support for critically ill patients in emergency care [6]. ICU resource allocation and admission protocols for patients should be observed meticulously by the medical organization and ought to be impartial and patient-centric [7]. Given that the multiplicity of virus mutations drastically affects the treatment handling approaches and the vaccination used for the treatment, data analysis based on mutation types, vaccinations, and treatment methods can help in understanding essential information and formulating strategic plans for future pandemics [8].

The interaction between COVID-19 and diabetes significantly impacts disease severity and has been explored in the literature through both traditional statistical analysis [9–12] and machine learning (ML) techniques [13,14]. With 19.1% of the population diagnosed with diabetes and 13.5% as prediabetic, Kuwait faces a considerable burden, making this investigation particularly relevant [15]. ML enhances the ability to strategically manage clinical research [16]. Multiple studies have identified risk factors for ICU admission associated with COVID-19 and employed ML techniques to develop models that predict disease severity based on data from laboratory tests, imaging, or clinical notes [17,18].

Imbalanced classification presents a challenge in predictive modeling due to skewed distributions favoring majority classes. This complicates modeling, as most ML algorithms assume equal representation across classes, rendering minority class predictions less reliable. Moreover, the minority class is often of greater importance and more susceptible to misclassification errors [19,20]. The Synthetic Minority Oversampling Technique (SMOTE) is a widely-used ML method that addresses this issue [21]. SMOTE creates a balanced dataset by oversampling minority instances, enhancing machine learning models' performance on imbalanced data using a simple and efficient augmentation technique [22].

This work examines the use of ML algorithms to create predictive models for ICU admission, using an extensive array of clinical and laboratory characteristics in COVID-19 patients, including variables that differentiate between those with and without diabetes. A prevalent issue in medical datasets is class imbalance, characterized by a substantial underrepresentation of one group (e.g., patients who need ICU care). This disparity may skew predictive models, resulting in erroneous forecasts, especially for the minority class. SMOTE is used to create synthetic samples in the feature space, thereby balancing the minority class and enhancing the model's fairness and precision. By using these methodologies, the analysis determines the most essential and informative variables. This research employed a feature selection strategy to identify the key predictors, since not all variables are necessary for precise predictions.

The Methods section provides a comprehensive description of the procedures employed, including SMOTE and feature selection techniques. Utilizing the Population, Intervention, Comparison, and Outcome (PICO) paradigm, the study questions were articulated as follows:

- **Q1:** How accurately can various ML models predict ICU admissions in patients diagnosed with COVID-19?
- **Q2:** Which important clinical and test factors, when added to a machine learning model, best predict whether a COVID-19 patient will need to go to the intensive care unit?

- **Q3:** In COVID-19 patients with diabetes, what are the differences in key variables predicting ICU admission compared to those identified for the general COVID-19 patient population?

This study was motivated by the urgent requirement of accurate and efficient predictive models designed for a specific demographic to improve healthcare responses. The primary contributions of this paper include:

- Dataset: A comprehensive and intricate dataset with demographic data and particular clinical results is presented, constituting one of the most exhaustive compilations of ICU needs during the COVID-19 epidemic in Kuwait.
- Feature Selection: To avoid the constraints of unrefined data, backward feature selection with logistic regression is used, enhancing the accuracy and efficacy of the prediction models. The research employs several ML techniques, including random forest (RF), extra trees (ET), support vector machine (SVM) with two kernels, logistic regression (LR), and decision tree (DT).
- Data Imbalance: Medical datasets often suffer from imbalanced data, which can distort model predictions. This challenge is addressed using SMOTE, ensuring balanced and fair model outcomes.
- Transparency: The model focuses on more than just forecasting; it also stresses interpretability. The Shapley Additive Explanations (SHAP) values show how important each predictor is, which helps us understand the ML results better, especially in a clinical setting.

The rest of this paper is divided into five sections. The background studies are explained in Section 2, followed by a detailed explanation of the methodology in Section 3. The data and model analysis are elaborated in Section 4 and then discussed in Section 5. Section 6 presents the study conclusions.

2. Background Studies

Effective patient care depends, inter alia, on precisely determining the necessity for intubation and on treatment timing. Deep learning and ML models, in particular, have become attractive answers to these problems, according to Ungar et al. [23], with several medical problems being strongly linked to children with COVID-19 being admitted to the ICU.

With an eye toward better patient care and outcomes, the work by Li et al. [24] presents a deep learning method to forecast the requirements for intubation in ICU patients. The model shows promising findings beyond conventional approaches, emphasizing the possibilities of artificial intelligence (AI) in healthcare environments. ML algorithms may lower uncertainty and ambiguity by offering empirical evidence for risk analyzers, examination, forecasting, and therapies, thus supporting reliable healthcare decisions and finally resulting in better patient results via superior levels of treatment [25].

The study conducted by Alkhunaizi et al. [26] investigates the effects of corticosteroid treatment on the clinical results of Saudi Arabia's patients with COVID-19 in the ICU. Their result demonstrates that corticosteroid medication is linked to lower death rates, shorter ICU stays, and a decreased requirement for mechanical ventilation. Also, their results endorse the utilization of corticosteroids in managing severe COVID-19 in ICU environments and offer significant perspectives for practical application. Table 1 presents a review of previous studies on the prediction of ICU admission.

Table 1. Overview of machine learning models utilized for predictive analysis in healthcare.

Reference and Year	Model	Target Type	Strength	Limitation
[27] 2024	XGB	Prediction of ICU admission and mortality with 1455 COVID-19 patients	The model achieved good performance with 88.56% accuracy	The study focused on imbalanced data and few hematological test records
[28] 2024	XGB	Prediction of ICU admission with 19,155 COVID-19 patients	The model's parameters were optimized utilizing simulated annealing and reached an AUC of 0.89	The study limits the generalizability of the model
[29] 2024	RF	Prediction of ICU mortality with 503 COVID-19 patients	The model achieved better results in mortality prediction with 81.42% accuracy	The study limits the generalizability of the model
[25] 2024	KNN	Prediction of mortality with 23 features for 696 COVID-19 patients	Different ML models were compared and achieved an accuracy of 95.25%	The study does not show the contribution of features and has challenges with missing data
[24] 2024	Deep neural network	Intubation in ICU patients with 55 variables	With an AUC score of 0.895, the study has strong predictive capabilities.	Data imbalance and complexity of the model may affect the performance
[30] 2023	Ensemble	In-hospital mortality of 1176 lung cancer patient	The model achieved an accuracy of 89% with a wide range of clinical features	The data contain missing values and limits the generalizability of the study
[31] 2023	LR	ICU transfer prediction with dichotomous variables for 532 COVID-19 patients	A robust feature selection for dichotomous variables with a 0.748 AUC score	The data were collected from a single hospital
[32] 2022	DT	Predicting intubation risk with 54 variables for 1225 COVID-19 patients	The model achieved an accuracy of 93.8% with an optimization algorithm	The data contain missing values and limits the generalizability of the study
[33] 2022	DT algorithms	ICU prediction with 53 variables for 512 COVID-19 patients	The model achieved an accuracy of 81.9% with external validation	The study only employed different DT algorithms
[34] 2022	ANN	Survival prediction of ICU with 64 variables for 326 COVID-19 patients	The model achieved an AUROC score of 0.917	Computationally intensive and requires more data
[35] 2022	CatBoost	Prediction of deterioration with 33 variables for 1079 COVID-19 patients	The model achieved an AUROC score of 0.84 and has performed external validation.	The dataset has more negative observations
[36] 2022	Light GB	Prediction of mortality for 1571 COVID-19 patients	The data includes a diverse population and achieved an AUC score of 0.88	Dataset size and missing data limit the generalizability of the study
[37] 2022	regression	Prediction of ICU admission and mortality for 793 pregnant COVID-19 patients	The model achieved an AUROC score of 0.73 and has developed a spreadsheet calculator for prediction	Missing data and lack of some maternal features may impact the model performance
[38] 2022	CART C5.0	Prediction of ICU admission for 228 Myasthenia gravis patients	The DT models enhance clinical decision-making with an AUC of 0.814	The data were collected from a single health center and has missing values
[39] 2021	Ensemble	Prediction of ICU admission and mortality for 5308 COVID-19 patients	High predictive performance with an F1-score of 0.81	The data contain missing values, imbalanced data, and limits the generalizability of the study
[12] 2021	LR	Prediction of mortality with 57 variables for 247 COVID-19 diabetic and prediabetic patients	The study was conducted across 10 hospitals and achieved an AUC score of 0.889	The study has not included a control group for non-diabetic patients

Table 1. *Cont.*

Reference and Year	Model	Target Type	Strength	Limitation
[40] 2021	Multivariable LR	Prediction of ICU admission and mortality for 356 COVID-19 patients	The model achieved an AUC score of 0.77 and employed a risk calculator	Dataset size and missing data limit the generalizability of the study
[41] 2021	RF	Prediction of ICU and ventilation for 212 COVID-19 patients	The model reduced the features to 5 key variables with an AUC of 0.80.	The data contain missing values, imbalanced data, and limits the generalizability of the study
[42] 2021	XGB	Prediction of ICU admission with 54 variables for 1925 COVID-19 patients	Different ML models were compared and achieved an AUC score of 0.98	Data were collected from a single health center and has challenges with missing data
[43] 2021	Ensemble	Prediction of ICU with CBC data for 1218 COVID-19 patients	The model achieved an AUC score of 0.88	Dataset size and missing data limit the generalizability of the study
[44] 2021	XGB	Prediction of ICU admission with 165 variables for 3623 COVID-19 patients	The model achieved an AUC of 0.83 and a web-based application was developed	The data were collected from a single health center
[14] 2020	CNN	Prediction of mortality for 9954 COVID-19 diabetic patients with clinical notes	The study used an advanced model and achieved an AUC score of 0.97	Computational complexity

AUC (area under the curve), CBC (complete blood count), DT (decision tree), CatBoost (categorical boosting), AUROC (area under the receiver operating characteristic curve), RF (random forest), GB (gradient boosting), XGB (extreme gradient boosting), ANN (artificial neural network), LR (logistic regression), and CART (classification and regression tree).

Although many studies provide important indicators of COVID-19 aspects, there is still the pressing need for a consistent approach to feature selection. Most of the models used several features, which might complicate clinical application. Moreover, the interpretation of features toward prediction was not evaluated in many studies. The difficulty of class imbalance, especially in mortality and ICU prediction models, has been reported in numerous studies.

3. Materials and Methods

3.1. Study Design

The use-case scenario illustrated in Figure 1 outlines the context of the study. It includes actors interacting with the system, its functionality, and the relationships between them. One key actor is the patient with COVID-19 who is admitted to the hospital, consulted by doctors, and tested for the virus. Doctors and nurses, as additional actors, record the patient's symptoms and clinical data. The medical records, which encompass ICU admission details, are stored in a database managed by an administrative entity. The "include" parameter in the connection links indicates a reliance on additional use cases to fulfill particular tasks. Patients are discharged following the physician's assessment.

After compiling the dataset, the machine learning model developer processes the data through cleaning, imputing, and standardization. The backward variable selection method is employed to select key medical variables. The model parameters are subsequently fine-tuned, and the optimal configuration is employed for training and validation. Finally, the trained model is implemented and deployed, ready to predict outcomes for new patient data in a clinical setting. This deployed model incorporates preprocessing steps, optimal variables, and the best ML model parameters for precise predictions.

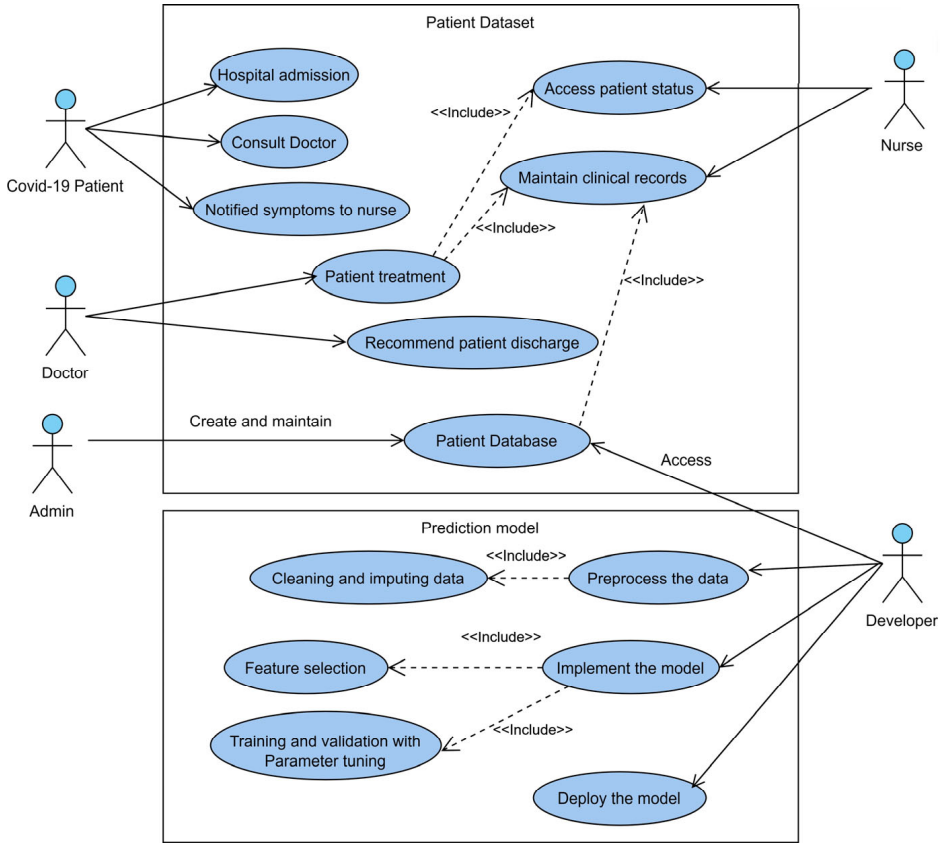

Figure 1. Use-case scenario.

3.2. The Dataset

Patients hospitalized in Kuwaiti hospitals between 4 May 2020 and 26 August 2020 were the subjects of the data collection. The appropriate legislative bodies authorized sample collection and patient surveys, and the Permanent Committee acquired the appropriate authorization forms for MHRC at the Ministry of Health (MOH). Patient data were gathered retrospectively, with the validation cohort's inclusion requirements necessitating the availability of admission and discharge information. Patients lacking this information were excluded from the validation group. All patients included in the study had tested positive for COVID-19 through polymerase chain reaction (PCR) testing.

Data were initially collected from 4555 patients, but 156 were excluded due to excessive missing values, leaving a final cohort of 4399 patients. The mean age of the participants was 42 years, with the interquartile range (Q1–Q3) extending from 31 to 54 years. Table 2 presents demographic information such as age and gender, as well as ICU admission criteria.

Table 2. Study cohort distribution by ICU admission, age, and gender.

Status	Age	Male	Female
ICU admission-required	Up to 30	7	1
	Between 31 and 50	97	6
	Between 51 and 65	91	18
	Above 65	46	15
ICU admission-not required	Up to 30	679	380
	Between 31 and 50	1371	489
	Between 51 and 65	569	302
	Above 65	173	155

The variables hypertension and diabetes mellitus (DM) were ascertained according to defined research conditions. Hypertension is characterized by a systolic blood pressure over 140 mmHg or a diastolic blood pressure surpassing 90 mmHg, with a value of 1 indicating hypertension and 0 indicating no hypertension. The glucose parameter represented random glucose levels in hospital patients, measured at any time of the day, not necessarily as a fasting sample. A patient was classified as having DM (value = 1) if their glucose level was $\geq$11.1 mmol/L or Hba1c was $\geq$6.5 mmol/L; otherwise, they were non-diabetic (DM value = 0). Patients with lower glucose levels but a positive history of DM were considered under medication [45].

Demographic predictors consisted of gender, age, height, and nationality. Symptoms recorded during COVID-19 included abdominal pain, fever, a history of bariatric surgery, asthma, headache, sore throat, expectoration, shortness of breath (SOB), weakness, diarrhea, and cough. Diabetes status during hospitalization was assessed through hemoglobin A1c (Hba1c), DM history, and glucose levels. Clinical testing incorporated lactate dehydrogenase (LDH), total bilirubin (T.Bili), respiratory rate, C-reactive protein (CRP), sodium (Na), serum albumin (S.Albumin), magnesium (Mg), prothrombin time, creatinine, alkaline phosphatase (ALP), temperature, pulse, carbon dioxide (CO_2), estimated glomerular filtration rate (eGFR), total protein (T.Protein), calcium (Ca), urate, gamma-glutamyl transferase (GGT), procalcitonin, ferritin, chloride (Cl), phosphate, activated partial thromboplastin clotting time (APTT), oximeter readings, alanine transaminase (ALT), international normalized ratio (INR), blood urea nitrogen (BUN), chest X-ray (CXR), D-dimer, and potassium (K).

Blood test parameters assessed included hematocrit (HCT), hemoglobin (HB), basophils (%), mean platelet volume (MPV), mean corpuscular volume (MCV), red blood cell (RBC) count, neutrophils (%), platelet count, white blood cell (WBC) count, mean cell hemoglobin concentration (MCHC), lactate dehydrogenase (LDH), lymphocytes (%), red cell distribution width (RDW), eosinophils (%), mean corpuscular hemoglobin (MCH), and monocytes (%). Table 3 provides a detailed description of each variable included in the study.

Table 3. The specifications of the COVID-19 dataset.

Variables	N	Missing Data		Mean ± Std. Deviation
		Count	%	
Eosinophil	4398	1	0	2.27 ± 2.50
LDH	3861	538	12.2	116.75 ± 406.87
RDW	4383	16	0.4	13.79 ± 2.34
Respiratory rate	1280	3119	70.9	21.96 ± 5.21
Diarrhea	1513	2886	65.6	-
Fever	1513	2886	65.6	-
Hypertension	1389	3010	68.4	-
BUN	4362	37	0.8	5.87 ± 7.52
DM	4299	100	2.3	-
Pulse oximetry	1355	3044	69.2	96.41 ± 4.95
Na	4356	43	1	137.70 ± 3.98
Hba1c	510	3889	88.4	8.94 ± 2.44
WBCs	4395	4	0.1	8.03 ± 4.74
Weakness	1513	2886	65.6	-
Creatinin	3908	491	11.2	96.22 ± 108.81
GGT	3975	424	9.6	45.13 ± 73.21
SBP	1389	3010	68.4	129.94 ± 18.17
DM history	1513	2886	65.6	-
Pulserate	1435	2964	67.4	87.77 ± 15.03
MCH	4384	15	0.3	27.14 ± 2.78
ALP	4321	78	1.8	82.87 ± 69.97
Nationality	4399	0	0	-
T.Bili	4160	239	5.4	14.38 ± 22.74
SOB	1513	2886	65.6	-

Table 3. *Cont.*

Variables	N	Missing Data		Mean ± Std. Deviation
		Count	%	
CXR	1462	2937	66.8	-
Phosphate	4258	141	3.2	1.28 ± 0.40
Mg	4209	190	4.3	0.83 ± 0.11
Bariatric Surgery	1513	2886	65.6	-
Urate	4179	220	5	297.94 ± 109.26
MCHC	4384	15	0.3	324.20 ± 17.47
Sore throat	1513	2886	65.6	-
Temp	1341	3058	69.5	37.04 ± 0.63
T.Protein	4288	111	2.5	65.12 ± 7.36
Lymphocytes	4380	19	0.4	26.01 ± 17.64
Neutrophils	4398	1	0	57.24 ± 16.18
Platelets count	4398	1	0	287.35 ± 117.14
Ferritin level	3805	594	13.5	102.52 ± 259.21
Prothrombin Time	3233	1166	26.5	14.14 ± 4.22
INR	3234	1165	26.5	1.05 ± 0.31
Glucose	4282	117	2.7	8.87 ± 5.10
APTT	3206	1193	27.1	33.46 ± 12.91
CL	4363	36	0.8	102.77 ± 5.53
Abdominal pain	1513	2886	65.6	-
Basophil	4384	15	0.3	0.44 ± 0.28
S.Albumin	4359	40	0.9	34.84 ± 7.41
RBCs	4398	1	0	4.78 ± 0.89
MCV	4384	15	0.3	83.60 ± 7.28
Procalcitonin	1470	2929	66.6	3.57 ± 28.46
Cough	1513	2886	65.6	-
DDimer	1223	3176	72.2	539.07 ± 1470.42
CO_2	4362	37	0.8	25.46 ± 3.13
Expectoration	1513	2886	65.6	-
CRP	2524	1875	42.6	32.89 ± 74.84
Monocytes	4384	15	0.3	8.79 ± 3.25
DBP	1388	3011	68.4	76.95 ± 10.97
Asthma	1513	2886	65.6	-
Age	4399	0	0	42.16 ± 16.73
Gender	4399	0	0	-
Ca	4269	130	3	2.23 ± 0.19
Headache	1513	2886	65.6	-
HB	4398	1	0	129.08 ± 23.76
ALT	4152	247	5.6	47.95 ± 216.65
HCT	4384	15	0.3	0.40 ± 0.07
MPV	4248	151	3.4	10.38 ± 1.77
eGFR	4043	356	8.1	97.17 ± 29.69
K	4353	46	1	4.27 ± 0.54
ICU admission	4399	0	0	

Abbreviations: ICU: Intensive Care Unit, WBC: White Blood Cell, MCHC: Mean Cell Hemoglobin Concentration, RBC: Red Blood Cell, MCH: Mean Corpuscular Hemoglobin, HB: Hemoglobin, HCT: Hematocrit, MCV: Mean Corpuscular Volume, Na: Sodium, K: Potassium, Cl: Chloride, Ca: Calcium, Mg: Magnesium, CO_2: Carbon Dioxide, SBP: Systolic Blood Pressure, CRP: C-Reactive Protein, T.Protein: Total Protein, T.Bili: Total Bilirubin, S.Albumin: Serum Albumin, LDH: Lactate Dehydrogenase, MPV: Mean Platelet Volume, DBP: Diastolic Blood Pressure, Hba1c: Hemoglobin A1c, DM: Diabetes Mellitus, CXR: Chest X-Ray, INR: International Normalized Ratio, BUN: Blood Urea Nitrogen, ALT: Alanine Transaminase, ALP: Alkaline Phosphatase, GGT: Gamma-Glutamyl Transferase, RDW: Red Cell Distribution Width, APTT: Activated Partial Thromboplastin Clotting Time, SOB: Shortness of Breath, eGFR: Estimated Glomerular Filtration Rate.

3.3. Methodology

This section elaborates on the method adopted in this study. The dataset includes 4399 records of COVID-19 patients, containing 66 variable columns that cover various demographic and clinical data. Initial preprocessing steps such as data cleaning, imputation, and normalization were performed to ensure the dataset's quality. Only the most

relevant and non-collinear variables identified were retained using techniques like Pearson correlation and chi-square tests. The dataset was then split into 60% for training and 40% as unseen data for testing.

SMOTE was utilized to mitigate class imbalances present in the training dataset. Various machine learning models were utilized on the processed data, specifically LR, SVM, DT, ET, and RF. A comprehensive evaluation was conducted utilizing 3-fold cross-validation (CV) alongside metrics including precision, recall, and F1-score, thereby ensuring a thorough and methodical analysis, as detailed in the following paragraphs.

Figure 2 presents the approach employed in this study. The dataset comprises multiple variables, including demographic information such as gender, age, and nationality, alongside COVID-19 symptoms, blood culture results, chronic diseases, oximeter readings, diabetes, pulse rate, and additional clinical findings, as outlined in Table 3. Preprocessing occurred before the application of classification models, and key variables were identified through a wrapper-based variable selection method.

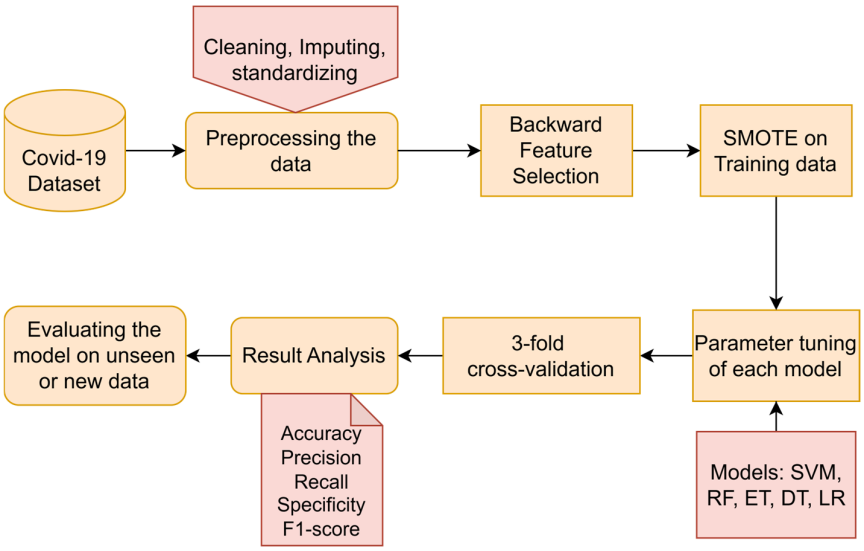

Figure 2. Study methodology.

3.4. Data Cleaning and Preprocessing

The initial stage involved cleaning the dataset to prepare it for modeling. Missing values were then addressed through an imputation method. Variables in Table 3 exhibiting over 75% missing values were omitted from the analysis [33]. The missing values were imputed using the K-nearest neighbors (KNN) method [46], an effective algorithm that utilizes Euclidean distance. This study established the number of neighbors at 5, the default value in the utilized package. This method substituted missing values with the mean of the five closest neighbors. The Euclidean distance is mathematically defined in Equation (1) as:

$$distance = \sqrt{weight * squared\ distance\ from\ f} \quad (1)$$

Here, f represents the current feature, and weight is determined as described in Equation (2) as:

$$weight = \frac{total\ number\ of\ features}{number\ of\ features\ having\ values} \quad (2)$$

Both missing and attributed data were analyzed to verify reliability. After addressing the missing values through the KNN method, the dataset underwent additional preprocessing to normalize all variables within a defined range.

3.5. Variable Selection

After excluding variables with more than 75% missing values, 65 independent variables and 1 target variable (ICU admission: 1 for required, 0 for not required) were retained. Utilizing all independent variables might have hindered the predictive performance of the ML models. To address this, highly correlated variables were identified and removed using Pearson correlation analysis for continuous variables, as illustrated in Figure 3. Variables with a correlation coefficient between 0.7 and 1 were considered strongly correlated, either positively or negatively [47].

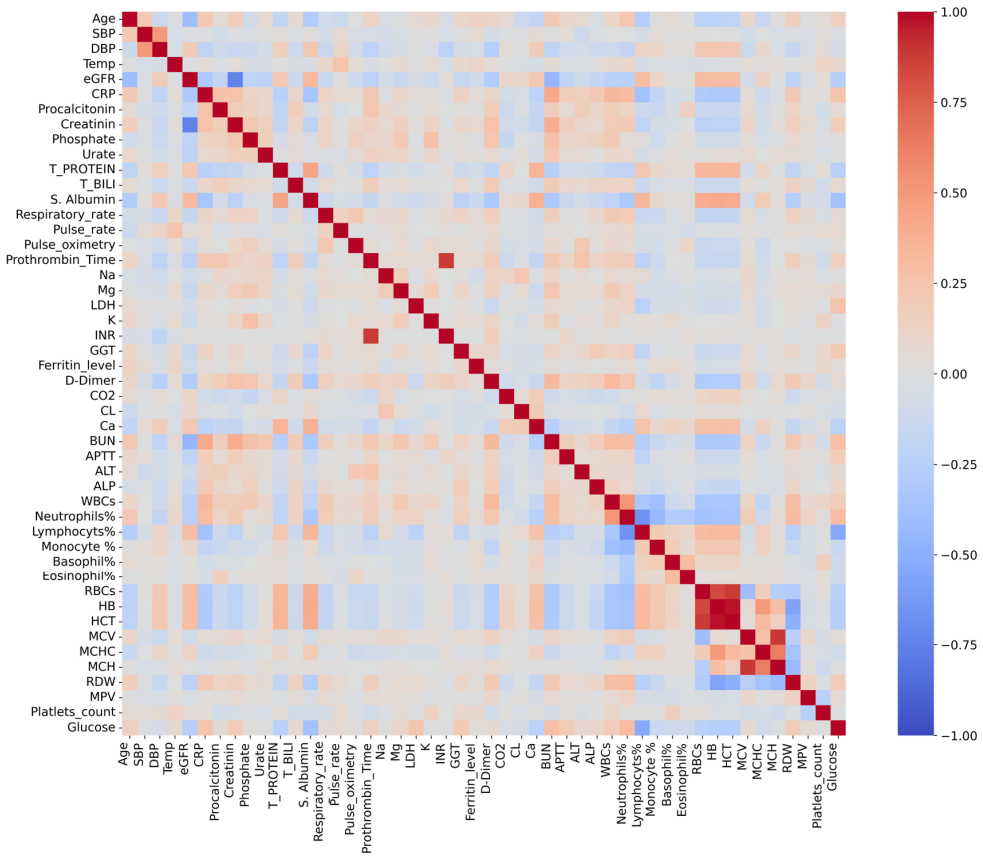

Figure 3. Correlation matrix of continuous variables. Toward the red color is positive correlation and toward the blue color is negative correlation.

A positive correlation indicates that both variables increase or decrease together, while a negative correlation signifies that one variable increases as the other decreases. Strong relationships were identified among several pairs of variables, including MCV-MCH, RBC-HCT, eGFR-creatinine, HB-HCT, prothrombin time-INR, and RBC-HB (as shown in Figure 3). These strongly correlated variables provided overlapping information, increasing the risk of overfitting in ML models. Accordingly, the variables MCV, HB, INR, RBC, and creatinine were removed from the dataset to enhance model performance and reduce redundancy.

The chi-square test for independence was employed to assess the association and significance of binary variables listed in Table 3. This test evaluated the relationship between independent variables, with the null hypothesis stating that there is no statistical difference between the observed variables. The null hypothesis is accepted when the p-value exceeds 0.05. The p-values for all binary variables are presented in Appendix A, Tables A1–A3. Variables such as headache, weakness, abdominal pain, history of bariatric surgery, diarrhea, and expectoration were removed from the dataset due to p-values greater than 0.05, indicating no significant difference among these variables.

For continuous data, a backward elimination wrapper method was used to identify relevant predictors [48,49]. LR was applied to determine the *p*-values of variables [50], assessing their contribution to predicting the target variable. The null hypothesis assumes no effect of the variable on the target outcome and is accepted when the *p*-value exceeds 0.05, leading to the variable's removal. For instance, if the variable "age" has a *p*-value of 0.001, it is deemed significant in predicting ICU admission and is retained for the classification model.

The flowchart in Figure 4 outlines the variable selection process, and the selected variables were used in the external validation test model. Detailed results from the logistic regression analysis are provided in Appendix A, Table A4.

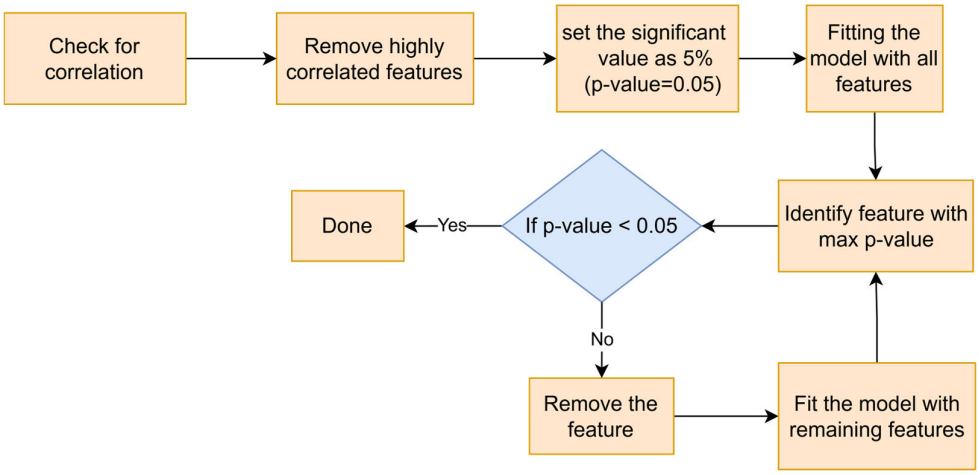

Figure 4. Flowchart depicting the variable selection process.

3.6. SMOTE and Parameter Tuning

The dataset with selected variables was processed using the train-test split method, with 60% of the data being employed for training and the remaining 40% kept as unseen data. Due to the imbalanced nature of the training data, the SMOTE technique was employed to address class imbalance. SMOTE generates additional instances for the minority class (ICU admission required) by interpolating existing positive samples within the variable space, improving model performance through oversampling. The performance of the ML models was assessed using a 3-fold CV method combined with a grid-search approach to optimize hyperparameters. The procedure partitions the dataset into three segments, utilizing two segments for model training and reserving the third for testing. The procedure was conducted thrice, ensuring each fold was utilized for testing once, with the final performance assessed by averaging the results across the folds.

The models were optimized using GridSearchCV with a 3-fold CV, and the best parameters for each classifier were selected based on accuracy scoring. Table 4 presents the tuned parameters for the models. The model with the best-tuned parameters was used for testing unseen data.

Table 4. Parameters of Machine Learning Models for Grid-Search with 3-Fold Cross-Validation.

Model Used	Tuning Parameters	The Range
DT	Max-depth Alpha	Range from 2 to 22 Range from 0.1 to 1×10^{-5}
SVM-Linear	tol C	Range from 0.1 to 1×10^{-5} Range from 2^{-1} to 2^{4}

Table 4. *Cont.*

Model Used	Tuning Parameters	The Range
RF	Max-features N-estimator	Auto, sqrt, log2 Range from 100 to 500
LR	tol C	Range from 0.1 to 1×10^{-5} 0.01, 0.1, 1, 2
SVM-RBF	Gamma C	Range from 2^{-2} to 2^{-5} From 2^{0} to 2^{4}
ET	Max-features N-estimator	Auto, sqrt, log2 Range from 100 to 500

3.7. Machine Learning Algorithms and Evaluation

This study utilized several machine learning algorithms, including DT, RF, and SVM with linear and radial basis function (RBF) kernels, LR, and ET models [51]. The best parameters were selected based on accuracy and subsequently used for evaluation on the dataset with stratified 3-fold CV, mitigating the risk of overfitting. Model bias and variance were also analyzed to ensure robustness. All analyses were implemented using Python and the Scikit-Learn library [52]. The pseudo-code of the study is shown in Figure 5.

Input: Patients' data with demographic, clinical records, and labels (ICU admission required)
Output: Classifying the ICU admission requirement

```
begin
    ⇨ Load and clean the data
    ⇨ Impute missing values using KNN imputer
    ⇨ Remove highly correlated variables
    ⇨ Perform feature selection
            For categorical features:
                Perform Chi-Square test
                Retain variables with significant association (p-value < 0.05)
            For continuous variables:
                Perform backward feature selection using Logistic Regression
    ⇨ Split the data into training (60%) and testing (40%) sets
    ⇨ Apply SMOTE on training data to balance the labels
    ⇨ Define the machine learning models
    ⇨ Set up hyperparameter grid for the model
    ⇨ Perform GridSearchCV with 3-fold cross-validation on the training data
            Identify the best model and hyperparameters
    ⇨ Evaluate the models with best parameter on the unseen 40% testing data
    ⇨ Calculate performance metrics
end
```

Figure 5. Pseudo-code of the study.

Model performance was evaluated using precision (positive predictive rate), recall (sensitivity), specificity, accuracy, and F1-score metrics. Accuracy provides an overall measure of model performance across classes but may be misleading in cases of imbalanced class distribution. For instance, when non-ICU admissions vastly outnumber ICU admissions, the model may predict all instances as non-ICU, overlooking actual ICU cases. Thus, additional metrics like recall, specificity, and F1-score were emphasized to provide a more nuanced evaluation of the model's performance. The evaluation equations are provided below:

$$Precision = \frac{trPs}{trPs + faPs} \tag{3}$$

$$Recall = \frac{trPs}{trPs + faNg} \tag{4}$$

$$F1 - Score = \frac{2trPs}{2trPs + faPs + faNg} \quad (5)$$

$$Accuracy = \frac{trPs + trNg}{trPs + trNg + faPs + faNg} \quad (6)$$

$$Specificity = \frac{trNg}{trNg + faPs} \quad (7)$$

where true positive (*trPs*), true negative (*trNg*), false positive (*faPs*), and false negative (*faNg*) are fundamental elements in calculating evaluation metrics. Precision measures the model's ability to accurately predict ICU admissions (the positive class) by minimizing false positives, ensuring that predictions of ICU admission are reliable. Recall assesses the model's capacity to identify all true ICU cases, with high recall indicating that the model successfully captures the majority of ICU patients. Specificity evaluates the model's effectiveness in correctly identifying non-ICU cases by minimizing false positives among negative instances, where high specificity reflects the model's reliability in recognizing non-ICU admissions. The F1-score represents the harmonic mean of precision and recall, balancing the trade-off between these two metrics to provide a comprehensive measure of model performance.

The receiver operating characteristic (ROC) curve is a valuable tool for assessing binary classification models. It plots the true positive rate against the false positive rate across various thresholds, offering insights into the model's performance. The area under the curve (AUC) serves as a summary metric, with values approaching 1 indicating superior model performance and more effective classification [53]. Additionally, SHAP was utilized to interpret the contributions of each variable to the predictions. SHAP provides detailed insights into how individual features influence model outcomes and is compatible with widely used ML libraries such as Scikit-Learn, TensorFlow, and PyTorch [54].

4. Results

4.1. Data Analysis

The dataset comprised a total of 4399 records, with 31% (1366) of the patients being female and 69% (3033) male. Among these, 281 patients (6%) required ICU admission, while 4118 (94%) did not. Missing values within the dataset were addressed using the KNN imputation method. The imputed and missing data were evaluated using the Hosmer–Lemeshow test within a logistic regression analysis. A *p*-value exceeding 0.05 supports the null hypothesis, demonstrating that the model adequately fits the data. Table 5 provides an analysis of missing and imputed data, indicating that the Hosmer–Lemeshow test validated a strong fit between the model and both datasets.

Table 5. Results of the Hosmer–Lemeshow Test for Goodness-of-Fit Analysis Considering Missing and Imputed Data.

The Dataset	df	Chi-Square	Sig. (*p*-Value)
With imputed	8	2.583	0.958
With missing	8	6.086	0.638

The data were standardized using the min-max function in Scikit-Learn, normalizing it based on the mean and variance of the dataset. Sixty percent of the data, comprising 2639 patient records, was allocated for training. Within this training dataset, the target label included 172 instances of ICU admission required and 2467 instances of ICU not required. Since under-sampling could result in the loss of valuable information, the SMOTE method was employed to address class imbalance. Over-sampling was applied to the minority class (ICU-required) to match the size of the majority class (ICU not required).

Parameter tuning was conducted using GridSearchCV, and the optimal parameters for each model were saved. Subsequently, the dataset was evaluated using a stratified 3-fold cross-validation approach, with each classifier being tested using its respective best parameters.

4.2. Variable Selection and Model Performance

The model was developed using 60% of the dataset based on the selected variables. To refine the variable set, highly correlated variables were excluded, and a backward elimination approach employing logistic regression was applied, as illustrated in Figure 4. This process reduced the number of variables from 65 to 20, based on their statistical significance (p-value < 0.05). Figure 6 shows the distribution of the selected predictors. The final variables included DM history, pulse rate, fever, T.Bili, respiratory rate, age, CXR, gender, MCHC, sore throat, D-dimer, LDH, T.Protein, WBCs, nationality, S.Albumin, DBP, SOB, pulse oximeter, and HCT.

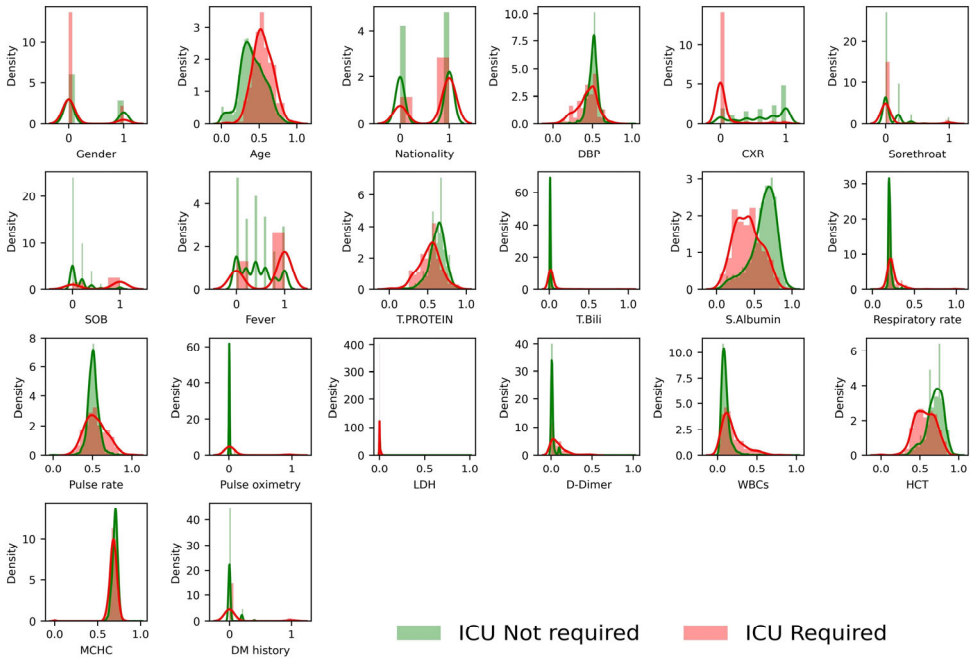

Figure 6. Distribution graph of chosen variables.

The models' parameters were tuned using GridSearchCV with 3-fold cross-validation, and the best parameters for each classifier were selected, as mentioned in Table 4. For the DT model, the optimal parameters were a max depth of 20 and an alpha of 1×10^{-3}. The SVM with the RBF kernel achieved the best accuracy with C = 2^4 and gamma = 2^{-2}. The optimal number of estimators was 100 for the ET classifier and 350 for the RF classifier, which also used max feature = log2. Similarly, the LR classifier was tuned with a regularization parameter of C = 2 and a tolerance value (tol) 1×10^{-3}. The SVM with the Linear kernel was trained using C = 2 and a tolerance value (tol) 0.0001.

Table 6 summarizes the evaluation results for all metrics of each ML model. All models underwent training and evaluation with their optimally tuned parameters. The ET classifier achieved the highest accuracy of 98.09%, exhibiting excellent performance in precision (0.9816), recall (sensitivity) (0.9809), F1-score (0.9813), and specificity (0.9809).

The confidence intervals (CIs) for each model are explained in Table 7. In addition to the metrics, 95% CI was calculated in this study to assess the reliability of the measures. CI is defined as:

$$CI = Mn \pm Z.\frac{\sigma}{\sqrt{s}} \tag{8}$$

where *Mn* is the mean of the metric (accuracy, precision, recall, and specificity), *Z* is the z-score of CI (which is 1.96), σ is the standard deviation of the metric, and *s* is the number of CV folds.

Table 6. Evaluation Metrics for All Models Utilizing 3-Fold Cross-Validation.

Model	Accuracy ± Std.	Precision ± Std.	Specificity ± Std.	F1-Score ± Std.	Recall ± Std.
LR	0.901 ± 0.022	0.901 ± 0.018	0.901 ± 0.022	0.901 ± 0.020	0.901 ± 0.022
DT	0.956 ± 0.014	0.957 ± 0.019	0.956 ± 0.019	0.956 ± 0.019	0.956 ± 0.019
SVM-RBF	0.959 ± 0.001	0.961 ± 0.024	0.959 ± 0.026	0.959 ± 0.025	0.959 ± 0.026
RF	0.974 ± 0.003	0.974 ± 0.016	0.974 ± 0.017	0.974 ± 0.016	0.974 ± 0.017
ET	0.981 ± 0.003	0.982 ± 0.017	0.981 ± 0.018	0.981 ± 0.018	0.981 ± 0.018
SVM-Linear	0.913 ± 0.001	0.914 ± 0.021	0.913 ± 0.026	0.913 ± 0.023	0.913 ± 0.026

Table 7. 95% CI for the performance measures of each training model.

Model	Accuracy	Precision	Specificity	F1-Score	Recall
LR	(0.876, 0.926)	(0.881, 0.921)	(0.876, 0.926)	(0.878, 0.924)	(0.876, 0.926)
DT	(0.940, 0.972)	(0.935, 0.979)	(0.934, 0.978)	(0.934, 0.978)	(0.934, 0.978)
SVM-RBF	(0.958, 0.960)	(0.934, 0.988)	(0.930, 0.988)	(0.931, 0.987)	(0.930, 0.988)
RF	(0.971, 0.977)	(0.956, 0.992)	(0.955, 0.993)	(0.956, 0.992)	(0.955, 0.993)
ET	(0.978, 0.984)	(0.963, 1.000)	(0.961, 1.000)	(0.961, 1.000)	(0.961, 1.000)
SVM-Linear	(0.912, 0.914)	(0.890, 0.938)	(0.884, 0.942)	(0.887, 0.939)	(0.884, 0.942)

The bias and variance of the CV models are illustrated in Figure 7. A low-bias model is prone to overfitting, leading to inaccurate predictions of new data, whereas a high-bias model tends to underfit, resulting in consistently poor predictions. Among the models, RF and ET, both ensemble models, exhibited the lowest variance, making them more stable compared to other models. The SVM model demonstrated a better fit for complex data distributions. Conversely, LR and SVM with a linear kernel exhibited increased bias, resulting in reduced sensitivity to noise within the dataset and lower accuracy on training data. Figure 8 illustrates the learning curve of the models, depicting misclassification error or loss throughout the training process.

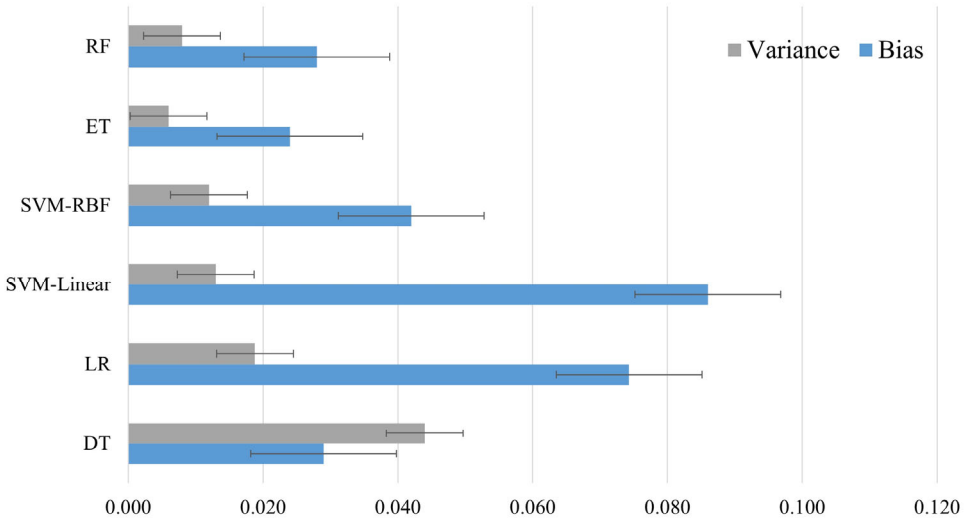

Figure 7. Misclassification errors in training and validation of models throughout the cross-validation process.

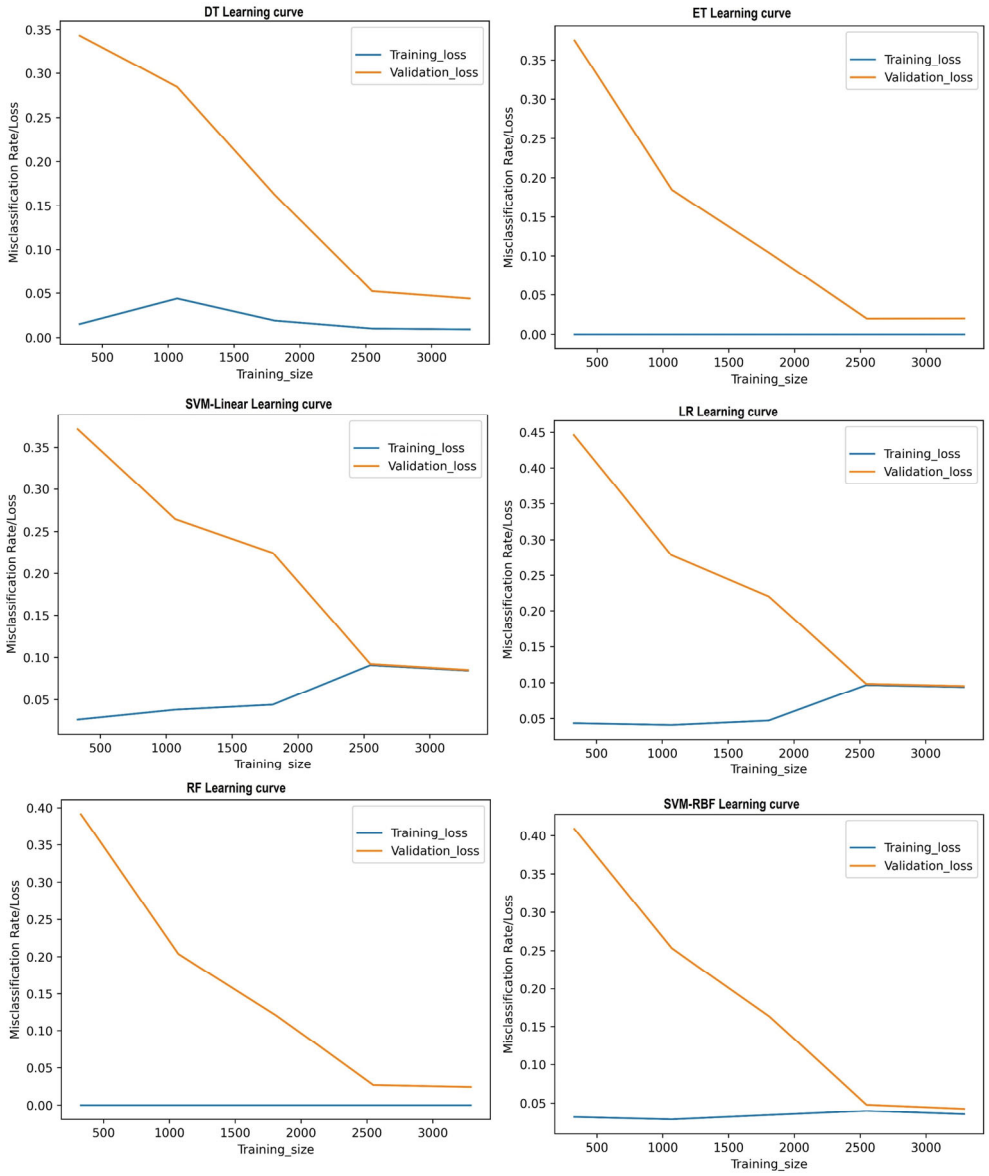

Figure 8. The learning curve of an appropriately fitted model.

The models with their best-tuned parameters were tested on external, unseen data comprising 40% of the original dataset, which comprised 1760 patient records. The SMOTE method was not applied to this test set, as real-world datasets are typically unbalanced, reflecting the natural distribution of data. The dataset in question exhibited an imbalance in the target variable, comprising 1651 instances where ICU admission was not required and 109 instances where ICU admission was required.

Given the imbalance, evaluation metrics such as recall (sensitivity), precision, F1-score, and specificity were used to assess model performance. The ET classifier achieved the highest accuracy at 96.42%, while LR and SVM models exhibited the highest precision values at 0.99. The complete evaluation results are presented in Table 8.

The ROC curve demonstrates the trade-off between true positives (sensitivity) and false positives across different classification thresholds. A higher AUC indicates a model's superior ability to differentiate between the two classes. Figure 9 displays the AUC scores for all machine learning models assessed on the unseen test data. The SVM-RBF and LR models attained the highest AUC scores, each at 0.91.

Table 8. External validation of the evaluated models using 40% of previously unseen imbalanced data.

Model	Accuracy	Precision	F1-Score	Recall	Specificity
DT	0.9290	0.9769	0.9616	0.9467	0.6606
RF	0.9574	0.9864	0.9771	0.9679	0.7982
LR	0.8972	0.9940	0.9423	0.8958	0.9174
ET	0.9642	0.9853	0.9808	0.9764	0.7798
SVM-RBF	0.9449	0.9905	0.9700	0.9503	0.8624
SVM-Linear	0.8989	0.9913	0.9435	0.9001	0.8807

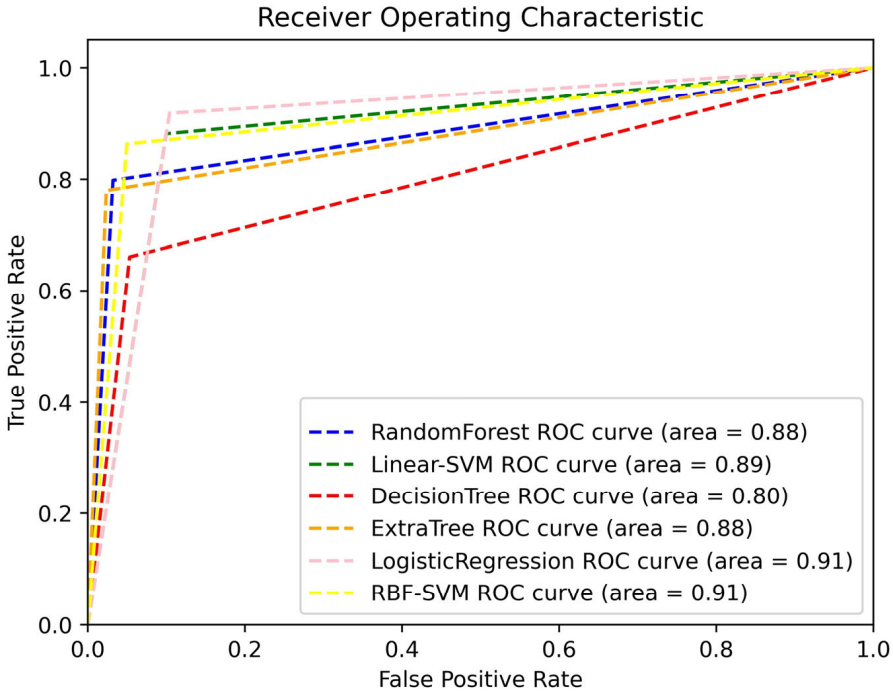

Figure 9. The receiver operating characteristic curve, along with the AUC score, is presented for the unseen test data.

The Friedman test was utilized to perform statistical significance testing across several ML models based on their metric values, followed by post-hoc analysis (In case accepted). The Friedman test is a non-parametric statistical method employed to identify variations in model performance. It is especially advantageous when the same datasets are employed for each study. The null hypothesis, which is accepted when the *p*-value is greater than 0.05, mentions that there is no difference in the metrics performance of all models. On the other hand, it is accepted when the *p*-value is less than 0.05, indicating at least one model has a different performance. The Friedman test shows a statistical value of 21.33 and a *p*-value of 0.00027. The average rank between each model is depicted in Table 9.

Table 9. Rank based on the Friedman test for statistical difference between each model.

Model	Accuracy	Precision	F1-Score	Recall	Specificity	AUC	Average Rank
DT	4	6	4	4	6	6	5
RF	2	4	2	2	4	4.5	3.08
LR	6	1	6	6	1	1.5	3.58
ET	1	5	1	1	5	4.5	2.92
SVM-RBF	3	3	3	3	3	1.5	2.75
SVM-Linear	5	2	5	5	2	3	3.67

The training and testing time of each model with feature selection is depicted in Table 10. Choosing a suitable model depending on the amount of the dataset and feature

dimensions requires knowledge of the computational complexity of the techniques. Although computing cost was considered, the primary focus of this study was obtaining the most accurate forecasts, especially considering the relevance of correct classification in ICU prediction.

Table 10. Computational complexity and training and testing time of each model with feature selection.

Model	Training Time (In Seconds)	Testing Time (In Seconds)	Time Complexity	Variables
DT	9.759	0.003	$O(f.s.\log(s))$	f = number of features s = number of samples t = number of trees E = epoch d = number of dimensions
RF	185.993	0.107	$O(t.f.s.\log(s))$	
ET	23.366	0.034	$O(t.f.s.\log(s))$	
LR	0.542	0.003	$O((f+1).s.E)$	
SVM-RBF	71.326	0.165	$O(s^2.d)$	
SVM-Linear	5.340	0.003	$O(s.d^2)$	

The models were also evaluated with full features. This helped to evaluate the impact of the feature selection methods employed in the study. The results are shown in Table 11. The best AUC is 0.89. Compared to this model with full features, there is an enhancement in the performance of models with feature selection (Table 8 and Figure 9). The AUC score, which is an effective evaluation metric for binary classification, shows that the model classifies ICU admission more precisely with the selected features rather than when utilizing full features.

Table 11. Training and testing results with full features.

Model	Training Accuracy	Training Time (In Seconds)	Testing Accuracy	Testing Time (In Seconds)	AUC
DT	0.9505	28.01	0.76	0.004	0.6473
RF	0.9594	293.98	0.96	0.095	0.7667
LR	0.9252	1.13	0.86	0.004	0.8924
ET	0.9613	30.18	0.96	0.052	0.8126
SVM-RBF	0.9377	74.48	0.94	0.122	0.7172
SVM-Linear	0.9291	9.96	0.87	0.004	0.8563

5. Discussion

This study aimed to predict ICU admission requirements in COVID-19 patients using selected clinical parameters. Variables were chosen through LR using a backward selection method, which reduces the dataset to the most relevant predictors. By eliminating redundant or unnecessary variables, this approach not only accelerates model training but also enhances performance and mitigates the risk of overfitting [55,56]. The final set of selected variables included age, DM history, CXR, pulse oximeter, WBCs, respiratory rate, fever, gender, D-dimer, sore throat, T.Protein, nationality, S.Albumin, HCT, LDH, DBP, MCHC, pulse rate, SOB, and T.Bili.

The missing values were imputed using a KNN imputer and the Hosmer–Lemeshow test (Table 5), which showed that the model remains strong with the imputed data. Further imputation analysis was performed on the missing dataset, which included dropping the missing values and evaluating the models, imputing the missing values with mean value, and constant value. The mean and constant values were implemented based on Simple Imputer from the Scikit-Learn library. The accuracy and AUC score of each model with different imputing methods are presented in Table 12. The KNN imputing method outperformed all the other methods tested, and the best result was SVM with a 0.91 AUC score (as mentioned in Figure 9).

Table 12. The performance of the models with different imputing methods (with selected features).

Model	Drop Missing		Mean Value		Constant Value	
	Accuracy (%)	AUC	Accuracy (%)	AUC	Accuracy (%)	AUC
DT	14	0.50	6	0.50	6	0.50
RF	14	0.50	6	0.50	6	0.50
LR	29	0.58	95	0.80	95	0.80
ET	29	0.58	7	0.50	12	0.53
SVM-RBF	43	0.67	87	0.83	87	0.83
SVM-Linear	21	0.33	95	0.82	95	0.88

The ET model exhibited exceptional performance, attaining an accuracy of 97.64% and an F1-score of 0.9808. The SVM-RBF model demonstrated superior precision and specificity, indicating a more conservative strategy in predicting ICU admissions. While the SVM-RBF model produced fewer false positives, it was more likely to miss some true positives compared to the ET model.

The AUC-ROC score was emphasized as a critical metric for evaluating the model's ability to distinguish between ICU admission requirements across all possible classification thresholds. Unlike metrics such as accuracy, recall, or specificity—which depend on a single threshold—the AUC-ROC score assesses the model's performance over a range of thresholds. This flexibility is particularly valuable in medical scenarios where the ideal decision threshold may vary depending on clinical priorities or ICU resource availability. The SVM-RBF model achieved the highest AUC score of 0.91, indicating its strong ability to differentiate ICU admission requirements irrespective of the threshold.

While the SVM-RBF model's accuracy (94.49%) was not the highest among the studied models, it did achieve an optimal balance between sensitivity (true positive rate) and specificity (true negative rate). SVM is widely recognized as a robust ML model [57]. Its ability to handle high-dimensional data and its resilience to overfitting make it well-suited for classification problems where classes are separable [58]. By identifying the optimal hyperplane, SVM effectively classifies data points even in complex distributions. The confusion matrix of the model used is depicted in Figure 10.

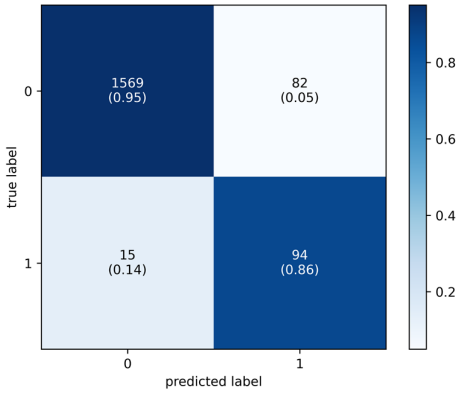

Figure 10. Confusion-matrix of the SVM-RBF model with selected features.

The choice of ML models, such as DT, RF, ET, and SVM, was influenced by the dataset size, problem characteristics, and variable sets [59]. Table 13 provides a comprehensive summary of previous studies that utilized these ML algorithms, further contextualizing this study's findings.

Table 13. Evaluation of machine learning models for forecasting ICU admissions.

Reference and Year	Model Used	Dataset	Best Results
[25] 2024	KNN	23 features and 696 COVID-19 patients	Accuracy is 95.25%
[31] 2023	LR	dichotomous variables with 532 COVID-19 patients	AUC = 0.748
[33] 2022	DT algorithm J-48	53 variables and 512 COVID-19 patients	Accuracy is 81.9%
[39] 2021	Ensemble model	5308 COVID-19 patients	F1-score is 0.81
[40] 2021	Multivariable LR	356 COVID-19 patients	AUC is 0.77
[41] 2021	RF	212 COVID-19 patients	AUC is 0.80
[43] 2021	Ensemble model	CBC data and 1218 COVID-19 patients	AUC is 0.88
[44] 2021	XGB	165 variables and 3623 COVID-19 patients	AUC is 0.83
[60] 2023	ANN	5 variables and 248 COVID-19 patients	Accuracy is 95.97%
Proposed Study	SVM-RBF	20 variables and 4399 COVID-19 patients	F1-score is 0.97 AUC is 0.91

The COVID-19 pandemic has posed significant challenges to the global healthcare sector, leading to shortages in ICU resources and healthcare workers. Developing AI-based systems to predict ICU admission requirements can assist healthcare providers in optimizing resource allocation. Numerous studies have explored ICU admission prediction, leveraging demographic information, blood test results, albumin levels, oxygen saturation, chronic disease history, and chest X-rays (CXR) to assess the need for intensive care [40,41,43,61]. Additionally, datasets updated during hospitalization have facilitated early risk detection [35]. Studies on mortality and survival predictions have identified critical predictors, including chloride, potassium, blood count tests, oxygen levels, D-dimer, and age, as significantly influencing outcomes [34,36,39,62].

Famiglini et al. [43] conducted a study utilizing SMOTE, focusing exclusively on blood count data as predictors. Their model employed an ensemble algorithm combining Extreme Gradient Boosting (XGB), RF, and LR classifiers, achieving an AUC score of 0.88. In another study, Shanbehzadeh et al. predicted ICU admission using a DT algorithm, resulting in an AUC of 0.822 [33]. The chi-square test was used to identify significant variables, with thromboplastin time, age, and diabetes emerging as top predictors. Age, oxygen saturation, pH, and chloride were also identified as significant factors for ICU admission in a separate study, where an artificial neural network (ANN) achieved an AUC of 0.917 [34].

For cases involving pregnant women, key variables such as body mass index (BMI), C-reactive protein (CRP), neutrophil percentage, and respiratory levels were identified as critical for predicting ICU admission [37]. Additionally, using a nomogram—a graphical calculation tool—the authors of another study [63] demonstrated effective ICU admission predictions based on five predictors: CRP, Lymphocytes count, aspartate transaminase (AST), lactate dehydrogenase (LDH), and platelet count.

Subudhi et al. [39] developed a prediction model using the RF classifier, incorporating critical markers such as C-reactive protein (CRP), clinical blood test results, oxygen levels, chloride, D-dimer, and procalcitonin. Some studies have demonstrated that the XGB algorithm performs better [42,44], achieving AUC scores of 0.98 and 0.83, respectively. High albumin levels in the body were also identified as a potential factor influencing ICU admission [64]. Additionally, patient factors such as diabetes mellitus (DM) history, gender, age, congestive heart failure (CHF), and stroke significantly contribute to prediction accuracy [65]. LR models have shown noteworthy predictive capabilities, with an AUC of 0.74 reported in one study [66], highlighting significant markers, including oxygen levels, procalcitonin, lymphocyte count, and lactate dehydrogenase (LDH). Deep learning models further enhance prediction by incorporating additional markers such as CRP and ferritin [67]. Moreover, rather than relying solely on clinical variables, another study [68] utilized scoring systems like the National Early Warning Score and Rapid Emergency Medicine Score to predict ICU admission effectively.

The SHAP plot shown in Figure 11 identifies the contribution of variables to the prediction of ICU admission. This analysis evaluates the 20 selected variables to determine their importance and impact on the target variable. The SHAP plot highlights the variables' importance and the nature of their influence—positive or negative—on ICU admission predictions. Variables with positive SHAP values positively influence the prediction of ICU admission, while negative SHAP values indicate the opposite.

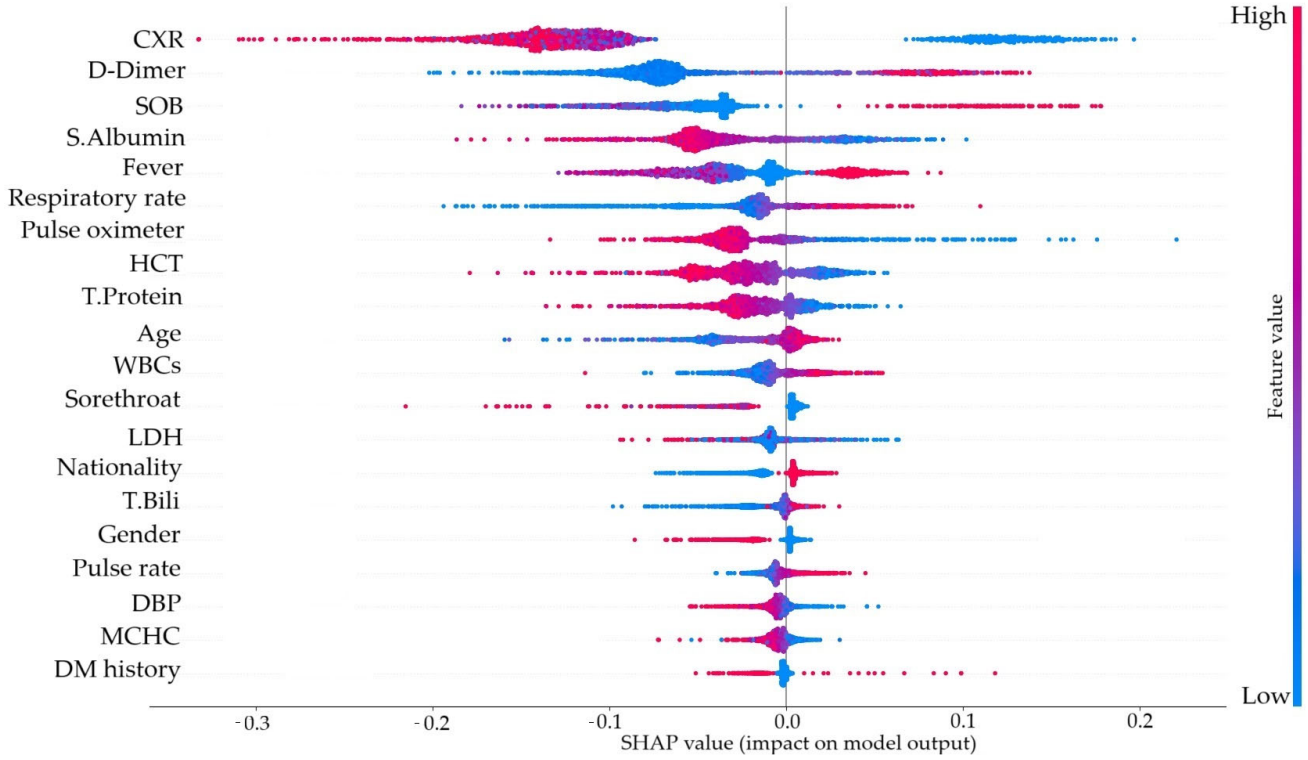

Figure 11. The SHAP value summary plot of the 20 most important variables for predicting ICU admission requirements.

The plot also visualizes variable contributions through color coding, where blue represents low values and red indicates high values. These colors demonstrate how variable values impact the prediction. The variables are arranged from most to least important, with the top three predictors being CXR, D-dimer, and SOB. A normal chest X-ray (coded as one) reduces the likelihood of ICU admission, while an abnormal X-ray (coded as zero) positively contributes to ICU predictions. Similarly, high values of D-dimer and SOB strongly favor ICU admission. For instance, a patient with a high D-dimer may be flagged for ICU admission when considered alongside other factors.

In contrast, variables such as T.Protein, sore throat, HCT, pulse oximeter, S.Albumin, LDH, gender, DBP, and MCHC negatively contribute to ICU admission when their values are high, indicating a lower need for ICU care. On the other hand, nationality, WBC, pulse rate, T.Bili, respiratory rate, fever, age, and DM history positively contribute to ICU admission when their values are elevated, suggesting a higher likelihood of requiring intensive care. This detailed variable analysis provides valuable insights into how specific clinical and demographic factors influence ICU admission prediction.

Certain illnesses and treatments require consideration of gender-specific information. For instance, men are more prone to cardiac conditions, while women commonly experience autoimmune disorders [69]. Gender inequalities in disease presentation and treatment choices, along with cultural norms and socioeconomic inequities, result in a complex environment that influences ICU utilization. Comprehending these factors is crucial for

formulating equitable healthcare policies and practices that address the clinical needs of all patients [70]. Age is another critical factor influencing the prevalence of various illnesses. Understanding a patient's nationality can also be essential in diagnosing or managing specific diseases or treatments. The organization and caliber of healthcare systems may differ markedly by nation, influencing ICU admission rates. In nations with well-established healthcare systems, patients may experience enhanced access to ICU treatment, whereas those in countries with underdeveloped systems may encounter obstacles that restrict their access.

High blood pressure increases the risk of heart disease, while CXR is valuable in diagnosing pneumonia and other respiratory disorders. Symptoms like fever, sore throat, and SOB may indicate infections, viruses, or allergic reactions. RBC breakdown releases bilirubin, while albumin is crucial in maintaining blood volume and pressure. Low levels of albumin and total protein, combined with elevated bilirubin, may signal kidney failure or liver disease.

Patients with elevated respiratory and pulse rates and low pulse oximeter readings often require ICU admission. High D-dimer levels can indicate the presence of blood clots. Increased LDH levels are associated with cell injury and linked to conditions such as cardiac arrest and stroke. Diabetes also heightens the risk of numerous health complications. Low HCT and MCHC levels can be indicative of anemia, whereas a high WBC count suggests an ongoing infection

The SHAP plot in Figure 11 indicates that non-Kuwaitis are more likely to require ICU admission, potentially due to economic, cultural, or other influencing factors. Differences in race and ethnicity among non-Kuwaitis, along with health disparities linked to environmental factors such as heat and air pollution, may contribute to this trend [71]. Additionally, this study aligns with the findings of Lat et al. [72], which shows that men are more likely to be admitted to an ICU compared to women. Both gender and nationality were found to have a significant impact on ICU admission outcomes in this study ($p < 0.001$). However, larger-scale studies are needed to confirm these results and further explore these associations, thus offering a potential area for future research and refinement.

The dataset was further divided based on random glucose levels to evaluate the model's performance in predicting ICU admission for diabetic and non-diabetic patients. This analysis examined how ICU requirements differed between the two groups. Among the COVID-19 patient records, 61% had low random glucose levels, while 39% had high values and were classified as diabetic.

For the diabetic dataset, the SVM-RBF model achieved an ICU prediction accuracy of 98.60%, while the non-diabetic dataset achieved 97.83% accuracy. The variable contributions to ICU admission prediction for diabetic patients are illustrated in Figure 12. The top 10 predictors for ICU admission among diabetic patients included high SOB, age, D-dimer, respiratory rate, low T.Protein, lymphocytes, CRP, low CXR values, and platelet count. These variables significantly influenced the predicted outcomes for diabetic patients.

This study has several notable strengths. First, the methodology effectively addresses key challenges: CV mitigates overfitting, while the SMOTE technique resolves class imbalance, ensuring accurate classification of both majority and minority classes. Second, the study incorporates a wide and comprehensive range of health-related data, including specific clinical and demographic details, for ICU admission prediction.

Variable importance and contribution are analyzed using the SHAP plot, providing valuable insights into each predictor's impact. Missing data are handled robustly through the KNN imputation method, maintaining dataset integrity. Additionally, backward variable elimination ensures that only the most relevant variables are included in the final prediction model, enhancing efficiency and accuracy.

The developed SVM model offers practical benefits by enabling timely alerts for healthcare workers to prepare ICU resources for COVID-19 patients. This proactive approach ensures that ICU resources are utilized effectively and efficiently, optimizing healthcare delivery during critical situations.

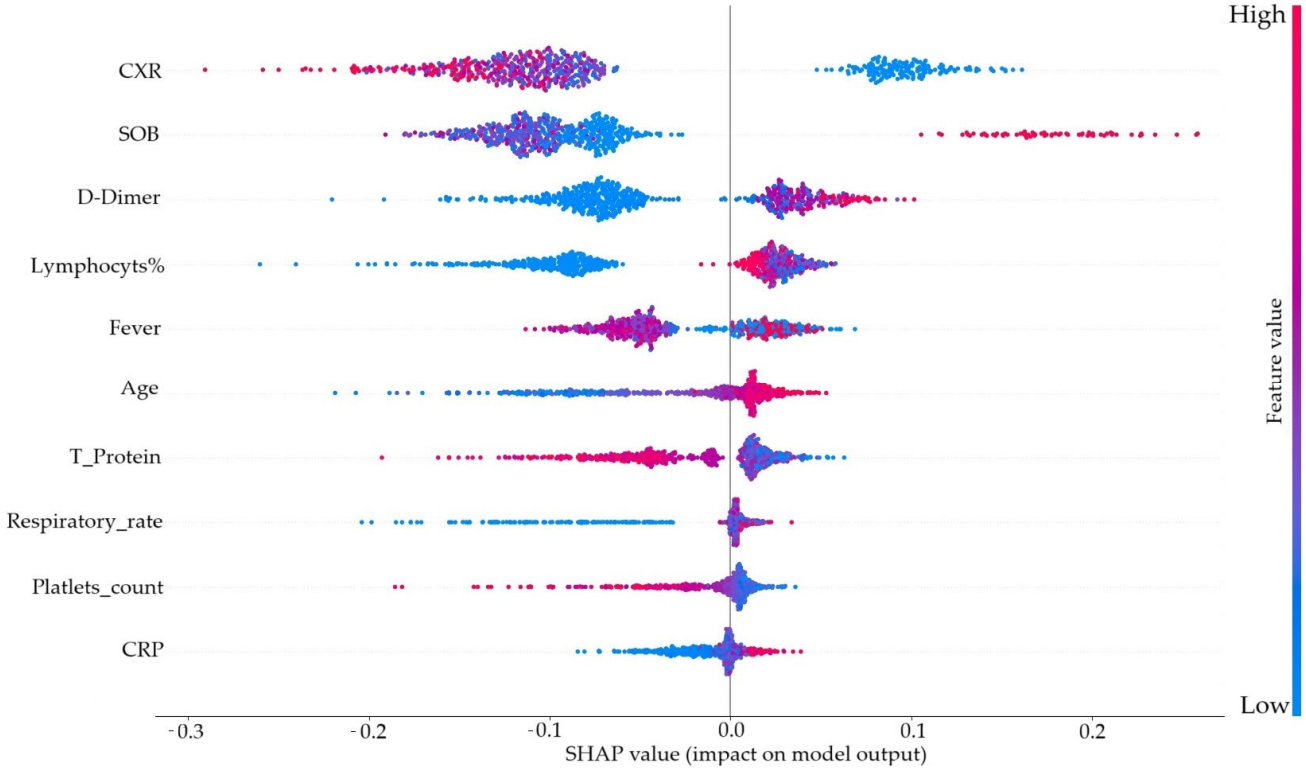

Figure 12. Variable importance for predicting ICU admission in the diabetic patient dataset.

5.1. Scalability of the Study

The proposed model shows a good foundation that can be scaled and modified for various illnesses and populations. The approaches utilized in the study can be extended to various infectious illnesses, chronic ailments, and acute medical situations. Data-driven methodologies could similarly be employed to forecast outcomes in illnesses such as influenza or pneumonia when prompt action is essential. Parameters such as age, comorbidities, and laboratory findings (e.g., blood glucose, D-dimer, LDH, WBC) are essential for predicting outcomes in patients with diabetes, heart disease, or other chronic conditions. This similarity enables the exchange of information and model frameworks across various health problems.

5.2. Practical Implications

The research formulated ML models to anticipate ICU admission needs for COVID-19 patients, and therefore possesses numerous practical implications for clinical practice, medical resource utilization, and further research endeavors. ICU physicians can use the SVM model for decision assistance. ICU admission projections in real time help healthcare practitioners make better patient management decisions, improving patient outcomes. Predicting which patients may need ICU hospitalization helps healthcare institutions allocate resources. ICU resources are scarce during health emergencies like COVID-19, making this aspect critical. Hospitals can better plan and assign manpower and equipment by identifying critical care patients earlier.

Training medical professionals on appropriate interpretation and application of the model's predictions is necessary. Knowing the outputs of the model and the clinical conse-

quences of the identified predictors, such as CXR, D-dimer levels, SOB, or S.Albumin findings, will enable doctors to make wiser judgments. This work concentrated on the model's creation and validation; nevertheless, its actual implementation necessitates more investigation, encompassing integration into hospital systems and healthcare provider training.

5.3. Limitations and Future Works

Future research will focus on implementing and comparing various feature selection methods, including filter, wrapper, and embedded techniques, to evaluate their influence on the performance and robustness of predictive models. Employing these diverse approaches aims to improve the accuracy and interpretability of the models, providing a more comprehensive understanding of variables' importance.

Additionally, a promising direction involves developing a model specifically based on data from Kuwaiti patients with diabetes to assess its clinical relevance within this high-risk group. This extension will evaluate the model's effectiveness in predicting ICU admission for diabetic patients, potentially enabling more personalized healthcare strategies and optimized resource allocation tailored to this vulnerable population.

Although it is typical of the COVID-19 patient group in Kuwaiti hospitals, the dataset used in our investigation is small. This limitation can influence the generalizability of our approach, especially concerning larger populations or other healthcare environments. Future studies should concentrate on combining other data sources, maybe from several healthcare facilities, to strengthen the dataset's resilience and guarantee that the model can be generalized properly over other demographic and or clinical situations.

6. Conclusions

This study utilized data from Kuwaiti hospitals to develop a predictive model for ICU admissions among COVID-19 patients. Advanced preprocessing techniques were applied, including class balancing with SMOTE, variable selection using backward elimination through logistic regression, and missing value imputation via KNN, validated by the Hosmer–Lemeshow test. The model demonstrated superior performance, with the SVM classifier achieving an AUC of 0.91 and an F1-score of 0.97.

In addition to identifying critical predictors for ICU admission, the study enhanced the interpretability of the machine learning model, aligning with the goals of discovery science to increase transparency in complex systems. The model's ability to assist effectively in ICU resource allocation during health crises underscores the potential of machine learning to augment healthcare responses and optimize resource utilization. This contribution represents a significant advancement in the fields of computational scientific discovery and intelligent data analysis.

The method facilitates the precise identification of patients at elevated risk for ICU admission, thereby offering essential assistance to healthcare professionals in making informed decisions about resource allocation. This highlights the broader applicability of machine learning-based models across scientific domains within discovery science. Ultimately, this work underscores the transformative role of machine learning in enabling scientific breakthroughs and enhancing healthcare strategies, offering promising advancements in both discovery science and practical healthcare applications.

Funding: This research received no external funding.

Institutional Review Board Statement: The study was approved by the Permanent Committee for Coordination of Medical and Health Research at the Ministry of Health, Kuwait, for sample collection and patient surveys with consent forms (Approval Number: 559, dated 3 May 2020).

Informed Consent Statement: Informed consent was obtained from all subjects involved in the study.

Data Availability Statement: The data required to reproduce the above findings cannot be shared for ethical reasons.

Acknowledgments: The author extends gratitude to all individuals who contributed to this study and to the clinicians from the hospitals in Kuwait for their invaluable support.

Conflicts of Interest: The author declares no conflicts of interest.

Appendix A

Table A1. Chi-square *p*-value for the association of independent categorical variables (Gender, Nationality, CXR, Weakness, Headache, Sore, Throat).

Variables	Gender	Nationality	CXR	Weakness	Headache	Sore Throat
Gender	-					
Nationality	<0.001	-				
CXR	0.006	<0.001	-			
Weakness	0.126	0.087	<0.001	-		
Headache	0.016	0.275	<0.001	<0.001	-	
Sore throat	<0.001	<0.001	<0.001	<0.001	<0.001	-
SOB	<0.001	<0.001	<0.001	<0.001	<0.001	<0.001
Abdominal pain	0.016	0.351	<0.001	<0.001	<0.001	0.255
Fever	<0.001	0.002	<0.001	<0.001	<0.001	<0.001
DM history	<0.001	0.004	<0.001	<0.001	0.151	<0.001
Diarrhea	<0.001	0.006	<0.001	<0.001	<0.001	<0.001
Cough	<0.001	0.002	<0.001	<0.001	<0.001	<0.001
Asthma	<0.001	<0.001	<0.001	<0.001	<0.001	<0.001
Hypertension	0.003	<0.001	<0.001	<0.001	<0.001	<0.001
Bariatric Surgery	0.015	0.122	0.316	<0.001	<0.001	<0.001
Expectoration	0.037	0.076	<0.001	<0.001	<0.001	<0.001
DM	<0.001	<0.001	<0.001	<0.001	0.032	<0.001

Table A2. Chi-square *p*-value for the association between independent categorical variables (SOB, Abdominal Pain, Fever, Expectoration, Diarrhea, Cough).

Variables	SOB	Abdominal Pain	Fever	Expectoration	Diarrhea	Cough
SOB	-					
Abdominal pain	$<1 \times 10^{-3}$	-				
Fever	$<1 \times 10^{-3}$	$<1 \times 10^{-3}$	-			
Expectoration	$<1 \times 10^{-3}$	0.601	$<1 \times 10^{-3}$	-		
Diarrhea	$<1 \times 10^{-3}$	$<1 \times 10^{-3}$	$<1 \times 10^{-3}$	1×10^{-3}	-	
Cough	$<1 \times 10^{-3}$	$<1 \times 10^{-3}$	$<1 \times 10^{-3}$	$<1 \times 10^{-3}$	$<1 \times 10^{-3}$	-
Asthma	$<1 \times 10^{-3}$	0.279	$<1 \times 10^{-3}$	1×10^{-3}	$<1 \times 10^{-3}$	$<1 \times 10^{-3}$
Bariatric Surgery	0.172	$<1 \times 10^{-3}$	$<1 \times 10^{-3}$	0.856	0.177	$<1 \times 10^{-3}$
Hypertension	$<1 \times 10^{-3}$	$<1 \times 10^{-3}$	$<1 \times 10^{-3}$	$<1 \times 10^{-3}$	$<1 \times 10^{-3}$	$<1 \times 10^{-3}$
DM history	$<1 \times 10^{-3}$	0.843	$<1 \times 10^{-3}$	$<1 \times 10^{-3}$	0.107	$<1 \times 10^{-3}$
DM	$<1 \times 10^{-3}$	0.026	$<1 \times 10^{-3}$	$<1 \times 10^{-3}$	0.269	$<1 \times 10^{-3}$

Table A3. Chi-square *p*-value for the association of independent categorical variables (Asthma, Bariatric Surgery, Hypertension, DM History).

Variables	Asthma	Bariatric Surgery	Hypertension	DM History
Asthma	-			
Bariatric Surgery	4×10^{-3}	-		
Hypertension	$<1 \times 10^{-3}$	0.033	-	
DM history	$<1 \times 10^{-3}$	0.991	$<1 \times 10^{-3}$	-
DM	$<1 \times 10^{-3}$	0.992	$<1 \times 10^{-3}$	$<1 \times 10^{-3}$

Table A4. Logistic regression results from the backward feature elimination method.

Variable	*p*-Value	Coef	Std Err	97% CI	
				Lower	Upper
Pulse oximeter	0	3.216	0.798	1.653	×0.428
Nationality	0	0.82	0.2	0.429	3.737
DM history	0	2.171	0.466	1.257	4.781
Gender	0	×0.887	0.235	×1.347	1.212
T.Protein	0	×2.509	0.69	×3.861	3.085
D-Dimer	0	4.441	1.16	2.168	×0.428
CXR	0	×3.277	0.43	×4.12	×1.158
Pulse rate	0.003	2.426	0.829	0.801	6.714
S.Albumin	0	×2.05	0.503	×3.036	×2.434
WBCs	0.005	2.425	0.862	0.735	4.052
Sore throat	0.002	×1.331	0.426	×2.165	×1.065
MCHC	0.003	×3.739	1.261	×6.212	4.116
LDH	0	×47.636	12.031	×71.216	×0.497
T.Bili	0.034	5.794	2.729	0.446	×1.267
DBP	0.01	×2.161	0.841	×3.811	×24.055
HCT	0.024	×1.778	0.789	×3.325	11.143
Fever	0.045	0.441	0.221	0.009	×0.513
Respiratory rate	0	6.185	1.703	2.847	×0.233
SOB	0	1.594	0.213	1.178	0.874
Age	0	2.528	0.617	1.319	9.524

References

1. Worldometer. COVID Live—Coronavirus Statistics. Available online: https://www.worldometers.info/coronavirus/ (accessed on 27 July 2022).
2. Supady, A.; Curtis, J.R.; Abrams, D.; Lorusso, R.; Bein, T.; Boldt, J.; Brown, C.E.; Duerschmied, D.; Metaxa, V.; Brodie, D. Allocating scarce intensive care resources during the COVID-19 pandemic: Practical challenges to theoretical frameworks. *Lancet Respir. Med.* **2021**, *9*, 430–434. [CrossRef] [PubMed]
3. Cascella, M.; Rajnik, M.; Aleem, A.; Dulebohn, S.; Di Napoli, R. Features, Evaluation, and Treatment of Coronavirus (COVID-19). Available online: https://www.statpearls.com/ArticleLibrary/viewarticle/52171 (accessed on 2 August 2023).
4. El-Sadr, W.M.; Vasan, A.; El-Mohandes, A. Facing the New COVID-19 Reality. *N. Engl. J. Med.* **2023**, *388*, 385–387. [CrossRef] [PubMed]
5. Foley, C.; Bloomer, M.; Hutchinson, A.M. Factors that influence intensive care admission decisions for older people: A systematic review. *Aust. Crit. Care* **2023**, *36*, 274–284. [CrossRef] [PubMed]
6. Olds, P.K.; Musinguzi, N.; Geisler, B.P.; Haberer, J.E. Evaluating disparities by social determinants in hospital admission decisions for patients with COVID-19 quaternary hospital early in the pandemic. *Medicine* **2023**, *102*, e33178. [CrossRef]
7. Valley, T.S.; Schutz, A.; Miller, J.; Miles, L.; Lipman, K.; Eaton, T.L.; Kinni, H.; Cooke, C.R.; Iwashyna, T.J. Hospital factors that influence ICU admission decision-making: A qualitative study of eight hospitals. *Intensive Care Med.* **2023**, *49*, 505–516. [CrossRef]
8. Miyashita, K.; Hozumi, H.; Furuhashi, K.; Nakatani, E.; Inoue, Y.; Yasui, H.; Karayama, M.; Suzuki, Y.; Fujisawa, T.; Enomoto, N.; et al. Changes in the characteristics and outcomes of COVID-19 patients from the early pandemic to the delta variant epidemic: A nationwide population-based study. *Emerg. Microbes Infect.* **2023**, *12*, 2155250. [CrossRef]
9. Alshukry, A.; Abbas, M.B.; Ali, Y.; Alahmad, B.; Al-Shammari, A.A.; Alhamar, G.; Abu-Farha, M.; AbuBaker, J.; Devarajan, S.; Dashti, A.A. Clinical characteristics and outcomes of COVID-19 patients with diabetes mellitus in Kuwait. *Heliyon* **2021**, *7*, e06706. [CrossRef]
10. Ali, H.; Al-Shammari, A.A.; Alahmad, B.; Al-Mulla, F. Advancing risk analysis of COVID-19 clinical predictors: The case of fasting blood glucose. *Front. Med.* **2021**, *8*, 636065. [CrossRef]
11. Dennis, J.M.; Mateen, B.A.; Sonabend, R.; Thomas, N.J.; Patel, K.A.; Hattersley, A.T.; Denaxas, S.; McGovern, A.P.; Vollmer, S.J. Type 2 Diabetes and COVID-19–Related Mortality in the Critical Care Setting: A National Cohort Study in England, March–July 2020. *Diabetes Care* **2020**, *44*, 50–57. [CrossRef]
12. Sourij, H.; Aziz, F.; Bräuer, A.; Ciardi, C.; Clodi, M.; Fasching, P.; Karolyi, M.; Kautzky-Willer, A.; Klammer, C.; Malle, O.; et al. COVID-19 fatality prediction in people with diabetes and prediabetes using a simple score upon hospital admission. *Diabetes Obes. Metab.* **2021**, *23*, 589–598. [CrossRef]
13. Anand, R.; Stey, P.; Jain, S.; Biron, D.; Bhatt, H.; Monteiro, K.; Feller, E.; Ranney, M.; Sarkar, I.; Chen, E. Predicting Mortality in Diabetic ICU Patients Using Machine Learning and Severity Indices. *AMIA Jt. Summits Transl. Sci. Proc.* **2018**, *2017*, 310–319. [PubMed]

14. Ye, J.; Yao, L.; Shen, J.; Janarthanam, R.; Luo, Y. Predicting mortality in critically ill patients with diabetes using machine learning and clinical notes. *BMC Med. Inform. Decis. Mak.* **2020**, *20*, 295. [CrossRef] [PubMed]
15. Alkandari, A.; Alarouj, M.; Elkum, N.; Sharma, P.; Devarajan, S.; Abu-Farha, M.; Al-Mulla, F.; Tuomilehto, J.; Bennakhi, A. Adult diabetes and prediabetes prevalence in Kuwait: Data from the cross-sectional Kuwait diabetes epidemiology program. *J. Clin. Med.* **2020**, *9*, 3420. [CrossRef] [PubMed]
16. Núñez Reiz, A.; Armengol de la Hoz, M.A.; Sánchez García, M. Big Data Analysis and Machine Learning in Intensive Care Units. *Med. Intensiv.* **2019**, *43*, 416–426. [CrossRef] [PubMed]
17. Cui, Y.; Zhou, Y.; Liu, C.; Mao, Z.; Zhou, F. Interpretable machine learning models for predicting the incidence of antibiotic-associated diarrhea in elderly ICU patients. *BMC Geriatr.* **2024**, *24*, 458. [CrossRef]
18. Xu, J.; Chen, T.; Fang, X.; Xia, L.; Pan, X. Prediction model of pressure injury occurrence in diabetic patients during ICU hospitalization—XGBoost machine learning model can be interpreted based on SHAP. *Intensive Crit. Care Nurs.* **2024**, *83*, 103715. [CrossRef]
19. Guo, X.; Yin, Y.; Dong, C.; Yang, G.; Zhou, G. On the Class Imbalance Problem. In Proceedings of the 2008 Fourth International Conference on Natural Computation, Shandong, China, 18–20 October 2008; pp. 192–201.
20. Johnson, J.M.; Khoshgoftaar, T.M. Survey on deep learning with class imbalance. *J. Big Data* **2019**, *6*, 27. [CrossRef]
21. Chawla, N.V.; Bowyer, K.W.; Hall, L.O.; Kegelmeyer, W.P. SMOTE: Synthetic minority over-sampling technique. *J. Artif. Intell. Res.* **2002**, *16*, 321–357. [CrossRef]
22. Fernández, A.; Garcia, S.; Herrera, F.; Chawla, N.V. SMOTE for learning from imbalanced data: Progress and challenges, marking the 15-year anniversary. *J. Artif. Intell. Res.* **2018**, *61*, 863–905. [CrossRef]
23. Ungar, S.P.; Solomon, S.; Stachel, A.; Shust, G.F.; Clouser, K.N.; Bhavsar, S.M.; Lighter, J. Hospital and ICU Admission Risk Associated with Comorbidities Among Children with COVID-19 Ancestral Strains. *Clin. Pediatr.* **2023**, *62*, 1048–1058. [CrossRef]
24. Li, R.; Xu, Z.; Xu, J.; Pan, X.; Wu, H.; Huang, X.; Feng, M. Predicting intubation for intensive care units patients: A deep learning approach to improve patient management. *Int. J. Med. Inform.* **2024**, *186*, 105425. [CrossRef] [PubMed]
25. Alie, M.S.; Negesse, Y.; Kassa, K.; Dereje Senay, M. Machine learning algorithms for predicting COVID-19 mortality in Ethiopia. *BMC Public Health* **2024**, *24*, 1728. [CrossRef] [PubMed]
26. Alkhunaizi, L.; Almutairi, J.A.; Almanea, S.H.; Alzahuf, S.M.; Fehaid, M.; Alharthi, A.; Tameem, A.; Alshuqayfi, S.M.; Alotaibi, R.; Alharbi, M.; et al. Impact of Corticosteroid Therapy on ICU Patient Outcomes in Severe COVID-19 Cases: A Retrospective Cohort Study in Saudi Arabia. *Cureus* **2024**, *16*, e53412. [CrossRef] [PubMed]
27. Molaei, S.; Moazen, H.; Niazkar, H.R.; Sabaei, M.; Johari, M.G.; Rezaianzadeh, A. Application of boosted trees to the prognosis prediction of COVID-19. *Health Sci. Rep.* **2024**, *7*, e2104. [CrossRef] [PubMed]
28. Ahmed, A.; Zengul, F.D.; Khan, S.; Hearld, K.R.; Feldman, S.S.; Hall, A.G.; Orewa, G.N.; Willig, J.; Kennedy, K. Developing a decision model to early predict ICU admission for COVID-19 patients: A machine learning approach. *Intell.-Based Med.* **2024**, *9*, 100136. [CrossRef]
29. Hamar, Á.; Mohammed, D.; Váradi, A.; Herczeg, R.; Balázsfalvi, N.; Fülesdi, B.; László, I.; Gömöri, L.; Gergely, P.A.; Kovacs, G.L. COVID-19 mortality prediction in Hungarian ICU settings implementing random forest algorithm. *Sci. Rep.* **2024**, *14*, 11941. [CrossRef]
30. Huang, T.; Le, D.; Yuan, L.; Xu, S.; Peng, X. Machine learning for prediction of in-hospital mortality in lung cancer patients admitted to intensive care unit. *PLoS ONE* **2023**, *18*, e0280606. [CrossRef]
31. Wendland, P.; Schmitt, V.; Zimmermann, J.; Häger, L.; Göpel, S.; Schenkel-Häger, C.; Kschischo, M. Machine learning models for predicting severe COVID-19 outcomes in hospitals. *Inform. Med. Unlocked* **2023**, *37*, 101188. [CrossRef]
32. Varzaneh, Z.A.; Orooji, A.; Erfannia, L.; Shanbehzadeh, M. A new COVID-19 intubation prediction strategy using an intelligent feature selection and K-NN method. *Inform. Med. Unlocked* **2022**, *28*, 100825. [CrossRef]
33. Shanbehzadeh, M.; Nopour, R.; Kazemi-Arpanahi, H. Using decision tree algorithms for estimating ICU admission of COVID-19 patients. *Inform. Med. Unlocked* **2022**, *30*, 100919. [CrossRef]
34. Rigo-Bonnin, R.; Gumucio-Sanguino, V.-D.; Pérez-Fernández, X.-L.; Corral-Ansa, L.; Fuset-Cabanes, M.; Pons-Serra, M.; Hernández-Jiménez, E.; Ventura-Pedret, S.; Boza-Hernández, E.; Gasa, M. Individual outcome prediction models for patients with COVID-19 based on their first day of admission to the intensive care unit. *Clin. Biochem.* **2022**, *100*, 13–21. [CrossRef] [PubMed]
35. Noy, O.; Coster, D.; Metzger, M.; Atar, I.; Shenhar-Tsarfaty, S.; Berliner, S.; Rahav, G.; Rogowski, O.; Shamir, R. A machine learning model for predicting deterioration of COVID-19 inpatients. *Sci. Rep.* **2022**, *12*, 2630. [CrossRef] [PubMed]
36. Kuno, T.; Sahashi, Y.; Kawahito, S.; Takahashi, M.; Iwagami, M.; Egorova, N.N. Prediction of in-hospital mortality with machine learning for COVID-19 patients treated with steroid and remdesivir. *J. Med. Virol.* **2022**, *94*, 958–964. [CrossRef] [PubMed]
37. Kalafat, E.; Prasad, S.; Birol, P.; Tekin, A.B.; Kunt, A.; Di Fabrizio, C.; Alatas, C.; Celik, E.; Bagci, H.; Binder, J. An internally validated prediction model for critical COVID-19 infection and intensive care unit admission in symptomatic pregnant women. *Am. J. Obstet. Gynecol.* **2022**, *226*, 403.e401–403.e413. [CrossRef] [PubMed]

38. Chang, C.-C.; Yeh, J.-H.; Chiu, H.-C.; Chen, Y.-M.; Jhou, M.-J.; Liu, T.-C.; Lu, C.-J. Utilization of Decision Tree Algorithms for Supporting the Prediction of Intensive Care Unit Admission of Myasthenia Gravis: A Machine Learning-Based Approach. *J. Pers. Med.* **2022**, *12*, 32. [CrossRef]
39. Subudhi, S.; Verma, A.; Patel, A.B.; Hardin, C.C.; Khandekar, M.J.; Lee, H.; McEvoy, D.; Stylianopoulos, T.; Munn, L.L.; Dutta, S. Comparing machine learning algorithms for predicting ICU admission and mortality in COVID-19. *NPJ Digit. Med.* **2021**, *4*, 87. [CrossRef]
40. Schalekamp, S.; Huisman, M.; van Dijk, R.A.; Boomsma, M.F.; Freire Jorge, P.J.; de Boer, W.S.; Herder, G.J.M.; Bonarius, M.; Groot, O.A.; Jong, E. Model-based prediction of critical illness in hospitalized patients with COVID-19. *Radiology* **2021**, *298*, E46–E54. [CrossRef]
41. Patel, D.; Kher, V.; Desai, B.; Lei, X.; Cen, S.; Nanda, N.; Gholamrezanezhad, A.; Duddalwar, V.; Varghese, B.; Oberai, A.A. Machine learning based predictors for COVID-19 disease severity. *Sci. Rep.* **2021**, *11*, 4673. [CrossRef]
42. Parbate, N.D.; Palande, A.P.; Wagh, S.K.; Kamble, A.; Isave, S. ICU Admission Prediction Using Machine Learning for Covid-19 Patients. In Proceedings of the 2021 International Conference on Communication information and Computing Technology (ICCICT), Mumbai, India, 25–27 June 2021; pp. 1–6.
43. Famiglini, L.; Bini, G.; Carobene, A.; Campagner, A.; Cabitza, F. Prediction of ICU admission for COVID-19 patients: A Machine Learning approach based on Complete Blood Count data. In Proceedings of the 2021 IEEE 34th International Symposium on Computer-Based Medical Systems (CBMS), Aveiro, Portugal, 7–9 June 2021; pp. 160–165.
44. Aznar-Gimeno, R.; Esteban, L.M.; Labata-Lezaun, G.; del-Hoyo-Alonso, R.; Abadia-Gallego, D.; Paño-Pardo, J.R.; Esquillor-Rodrigo, M.J.; Lanas, Á.; Serrano, M.T. A clinical decision web to predict ICU admission or death for patients hospitalised with COVID-19 using machine learning algorithms. *Int. J. Environ. Res. Public Health* **2021**, *18*, 8677. [CrossRef]
45. Committee, A.D.A.P.P. 2. Classification and Diagnosis of Diabetes: Standards of Medical Care in Diabetes—2022. *Diabetes Care* **2021**, *45*, S17–S38. [CrossRef]
46. Troyanskaya, O.; Cantor, M.; Sherlock, G.; Brown, P.; Hastie, T.; Tibshirani, R.; Botstein, D.; Altman, R.B. Missing value estimation methods for DNA microarrays. *Bioinformatics* **2001**, *17*, 520–525. [CrossRef] [PubMed]
47. Ratner, B. The correlation coefficient: Its values range between+ 1/− 1, or do they? *J. Target. Meas. Anal. Mark.* **2009**, *17*, 139–142. [CrossRef]
48. Mehmood, M.; Alshammari, N.; Alanazi, S.A.; Ahmad, F. Systematic Framework to Predict Early-Stage Liver Carcinoma Using Hybrid of Feature Selection Techniques and Regression Techniques. *Complexity* **2022**, *2022*, 7816200. [CrossRef]
49. Park, J.; Li, K.; Zhou, H. k-fold Subsampling based Sequential Backward Feature Elimination. In Proceedings of the International Conference on Pattern Recognition Applications and Methods (ICPRAM), Rome, Italy, 24–26 February 2016; pp. 423–430.
50. Nick, T.G.; Campbell, K.M. Logistic Regression. In *Topics in Biostatistics*; Ambrosius, W.T., Ed.; Humana Press: Totowa, NJ, USA, 2007; pp. 273–301.
51. Kumari, R.; Srivastava, S.K. Machine learning: A review on binary classification. *Int. J. Comput. Appl.* **2017**, *160*. [CrossRef]
52. Pedregosa, F.; Varoquaux, G.; Gramfort, A.; Michel, V.; Thirion, B.; Grisel, O.; Blondel, M.; Prettenhofer, P.; Weiss, R.; Dubourg, V. Scikit-learn: Machine learning in Python. *J. Mach. Learn. Res.* **2011**, *12*, 2825–2830.
53. Fan, J.; Upadhye, S.; Worster, A. Understanding receiver operating characteristic (ROC) curves. *Can. J. Emerg. Med.* **2006**, *8*, 19–20. [CrossRef]
54. Lundberg, S.M.; Lee, S.-I. A unified approach to interpreting model predictions. *arXiv* **2017**, arXiv:1705.07874. [CrossRef]
55. Mahalakshmi, K.; Sujatha, P. Critical Analysis of Feature Selection Methods for Data Preprocessing with Heart Disease Dataset. In *Data Intelligence and Cognitive Informatics*; Springer: Berlin/Heidelberg, Germany, 2022; pp. 667–682.
56. Bharathi, N.; Rishiikeshwer, B.; Shriram, T.A.; Santhi, B.; Brindha, G. The Significance of Feature Selection Techniques in Machine Learning. In *Fundamentals and Methods of Machine and Deep Learning: Algorithms, Tools and Applications*; Scrivener Publishing LLC: Austin, TX, USA, 2022; pp. 121–134.
57. Yue, S.; Li, P.; Hao, P. SVM classification: Its contents and challenges. *Appl. Math. J. Chin. Univ.* **2003**, *18*, 332–342. [CrossRef]
58. Yang, Y.; Li, J.; Yang, Y. The research of the fast SVM classifier method. In Proceedings of the 2015 12th International Computer Conference on Wavelet Active Media Technology and Information Processing (ICCWAMTIP), Chengdu, China, 18–20 December 2015; pp. 121–124.
59. Fernández-Delgado, M.; Cernadas, E.; Barro, S.; Amorim, D. Do we need hundreds of classifiers to solve real world classification problems? *J. Mach. Learn. Res.* **2014**, *15*, 3133–3181.
60. Asteris, P.G.; Kokoris, S.; Gavriilaki, E.; Tsoukalas, M.Z.; Houpas, P.; Paneta, M.; Koutzas, A.; Argyropoulos, T.; Alkayem, N.F.; Armaghani, D.J. Early prediction of COVID-19 outcome using artificial intelligence techniques and only five laboratory indices. *Clin. Immunol.* **2023**, *246*, 109218. [CrossRef]
61. Mushtaq, J.; Pennella, R.; Lavalle, S.; Colarieti, A.; Steidler, S.; Martinenghi, C.; Palumbo, D.; Esposito, A.; Rovere-Querini, P.; Tresoldi, M. Initial chest radiographs and artificial intelligence (AI) predict clinical outcomes in COVID-19 patients: Analysis of 697 Italian patients. *Eur. Radiol.* **2021**, *31*, 1770–1779. [CrossRef] [PubMed]

62. Ayed, M.; Borahmah, A.A.; Yazdani, A.; Sultan, A.; Mossad, A.; Rawdhan, H. Assessment of clinical characteristics and mortality-associated factors in COVID-19 critical cases in Kuwait. *Med. Princ. Pract.* **2021**, *30*, 185–192. [CrossRef] [PubMed]
63. Zeng, Z.; Ma, Y.; Zeng, H.; Huang, P.; Liu, W.; Jiang, M.; Xiang, X.; Deng, D.; Liao, X.; Chen, P. Simple nomogram based on initial laboratory data for predicting the probability of ICU transfer of COVID-19 patients: Multicenter retrospective study. *J. Med. Virol.* **2021**, *93*, 434–440. [CrossRef]
64. Kheir, M.; Saleem, F.; Wang, C.; Mann, A.; Chua, J. Higher albumin levels on admission predict better prognosis in patients with confirmed COVID-19. *PLoS ONE* **2021**, *16*, e0248358. [CrossRef]
65. Gunduz, R.; Yildiz, B.S.; Ozdemir, I.H.; Cetin, N.; Ozen, M.B.; Bakir, E.O.; Ozgur, S.; Bayturan, O. CHA2DS2-VASc score and modified CHA2DS2-VASc score can predict mortality and intensive care unit hospitalization in COVID-19 patients. *J. Thromb. Thrombolysis* **2021**, *52*, 914–924. [CrossRef]
66. Zhao, Z.; Chen, A.; Hou, W.; Graham, J.M.; Li, H.; Richman, P.S.; Thode, H.C.; Singer, A.J.; Duong, T.Q. Prediction model and risk scores of ICU admission and mortality in COVID-19. *PLoS ONE* **2020**, *15*, e0236618. [CrossRef]
67. Li, X.; Ge, P.; Zhu, J.; Li, H.; Graham, J.; Singer, A.; Richman, P.S.; Duong, T.Q. Deep learning prediction of likelihood of ICU admission and mortality in COVID-19 patients using clinical variables. *PeerJ* **2020**, *8*, e10337. [CrossRef]
68. Covino, M.; Sandroni, C.; Santoro, M.; Sabia, L.; Simeoni, B.; Bocci, M.G.; Ojetti, V.; Candelli, M.; Antonelli, M.; Gasbarrini, A. Predicting intensive care unit admission and death for COVID-19 patients in the emergency department using early warning scores. *Resuscitation* **2020**, *156*, 84–91. [CrossRef]
69. Todorov, A.; Kaufmann, F.; Arslani, K.; Haider, A.; Bengs, S.; Goliasch, G.; Zellweger, N.; Tontsch, J.; Sutter, R.; Buddeberg, B.; et al. Gender differences in the provision of intensive care: A Bayesian approach. *Intensive Care Med.* **2021**, *47*, 577–587. [CrossRef]
70. Kotfis, K.; Olusanya, S.; Modra, L. Equity in patient care in the intensive care unit. *Intensive Care Med.* **2024**, *50*, 291–293. [CrossRef]
71. Alahmad, B.; Shakarchi, A.F.; Khraishah, H.; Alseaidan, M.; Gasana, J.; Al-Hemoud, A.; Koutrakis, P.; Fox, M.A. Extreme temperatures and mortality in Kuwait: Who is vulnerable? *Sci. Total Environ.* **2020**, *732*, 139289. [CrossRef] [PubMed]
72. Lat, T.I.; McGraw, M.K.; White, H.D. Gender Differences in Critical Illness and Critical Care Research. *Clin. Chest Med.* **2021**, *42*, 543–555. [CrossRef] [PubMed]